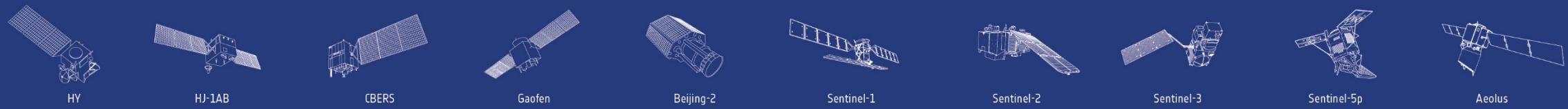

2023 DRAGON 5 SYMPOSIUM

3rd YEAR RESULTS REPORTING

11-15 SEPTEMBER 2023

PROJECT ID. 59307

3-D CHARACTERIZATION AND TEMPORAL ANALYSIS OF FORESTS AND VEGETATED AREAS USING TIME-SERIES OF POLARIMETRIC SAR DATA AND TOMOGRAPHIC PROCESSING

THURSDAY, 14 SEPT. 2024

ID. 192

PROJECT TITLE: 3-D CHARACTERIZATION AND TEMPORAL ANALYSIS OF FORESTS AND VEGETATED AREAS USING TIME-SERIES OF POLARIMETRIC SAR DATA AND TOMOGRAPHIC PROCESSING

PRINCIPAL INVESTIGATORS: LAURENT FERRO-FAMLI

CO-AUTHORS: ERXUE CHEN, ZENGYUAN LI, ZHAO LEI
WEN HONG, QIANG YIN,
XINWU LI, XING PENG,
THUY LE TOAN

PRESENTED BY: ERXUE CHEN

Outlines

1. **Project's objectives**
2. **Mission data utilised**
3. **Field data collection campaigns**
4. **Results after 3 years of activity**
5. **Schedule, planning & contribution of 2024**
6. **Training of young scientists**
7. **Peer reviewed publications**

1. Project's objectives

- **Promote the use of existing spaceborne SAR sensors with polarimetric and interferometric diversities for the temporal monitoring of forested and vegetated areas and to pave the way for future spaceborne missions and concepts.**

  - **Development of physical parameter retrieval methods for the quantitative 3-D characterization of forest areas using low frequency sensors;**
  - **Development of innovative vector signal processing techniques for high-resolution 3-D imaging;**
  - **Temporal monitoring of forested and vegetated areas using time-series of acquisitions;**
  - **Updating PolSARpro Software.**

2. Mission data utilised

Data access (list all missions and issues if any). NB. in the tables please insert cumulative figures (since July 2020) for no. of scenes of high bit rate data (e.g. S1 100 scenes). If data delivery is low bit rate by ftp, insert “ftp”

ESA /Third Party Missions	No. Scenes
1. Sentinel 1	100s
2. GEDI	10s
3. ESA Airborne campaigns	10s
4. UAV SAR	10s
Total:	100 s
Issues:	

Chinese EO data	No. Scenes
1. CASMSAR	200+
2.	
3.	
4.	
5.	
6.	
Total:	200+
Issues:	

3. Field data collection campaigns

- **Genhe, Inner Mongolia (P/L/S/C/X, 2021.09)**
  - PolSAR data, where the C-band is acquired in the dual-antenna PolInSAR mode.
  - TomoSAR data, each band acquired more than 10 tracks of data.
  - Airborne LiDAR and in situ data.

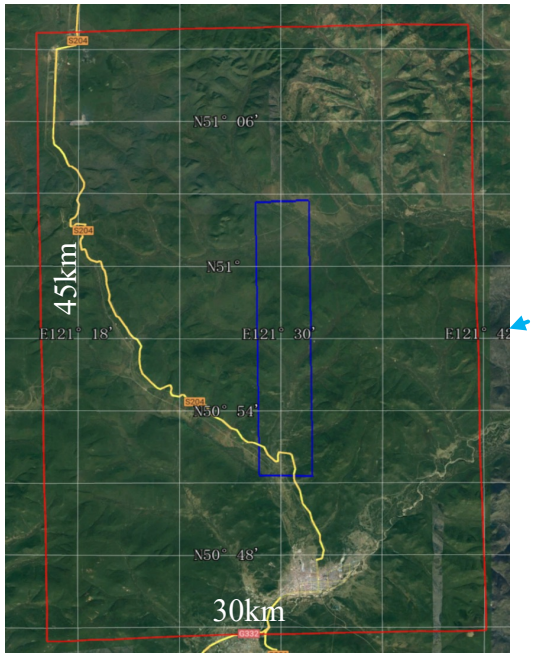

- **Zhaoqing, Guangdong Province (PSAR, 2022.09)**
  - TomoSAR data, observing by flying in 4 directions
  - About 16 or 17 tracks for each observation direction
  - Forest plot data collection planned in Sept. of 2023

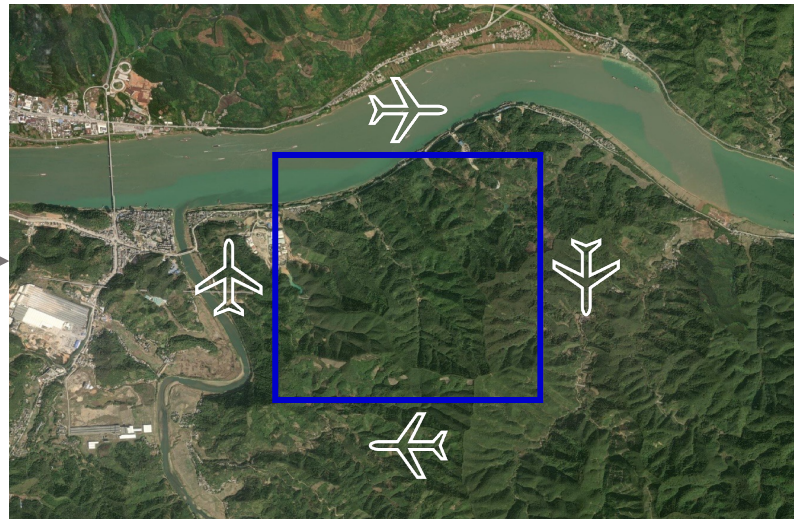

4. Results after 3 years of activity

4.1 Assessment of High-resolution Airborne Multi-band PolSAR to Estimate Forest Stem Volume

4.2 Forest height and AGB estimation from X- and P-band InSAR data

4.3 A new approach of phase calibration for TomoSAR over forested area

4.4 TomoSAR—Forest underlying topography estimation

4.5 TomoSAR——Building height estimation

4.6 Preparation of ESA's BIOMASS mission

4.7 PolSAR image Classification Based on Polarimetric-Temporal Feature Selection

4.8 PolSAR image Classification Based on Time-Variant Features from T matrix operation in time dimension

4.9 Near-Real Time deforestation monitoring using S1

4.1 Assessment of High-resolution Airborne Multi-band PolSAR to Estimate Forest Stem Volume

■ The sensitivity of P/L/S/C/X SAR backscatter intensity to stem volume

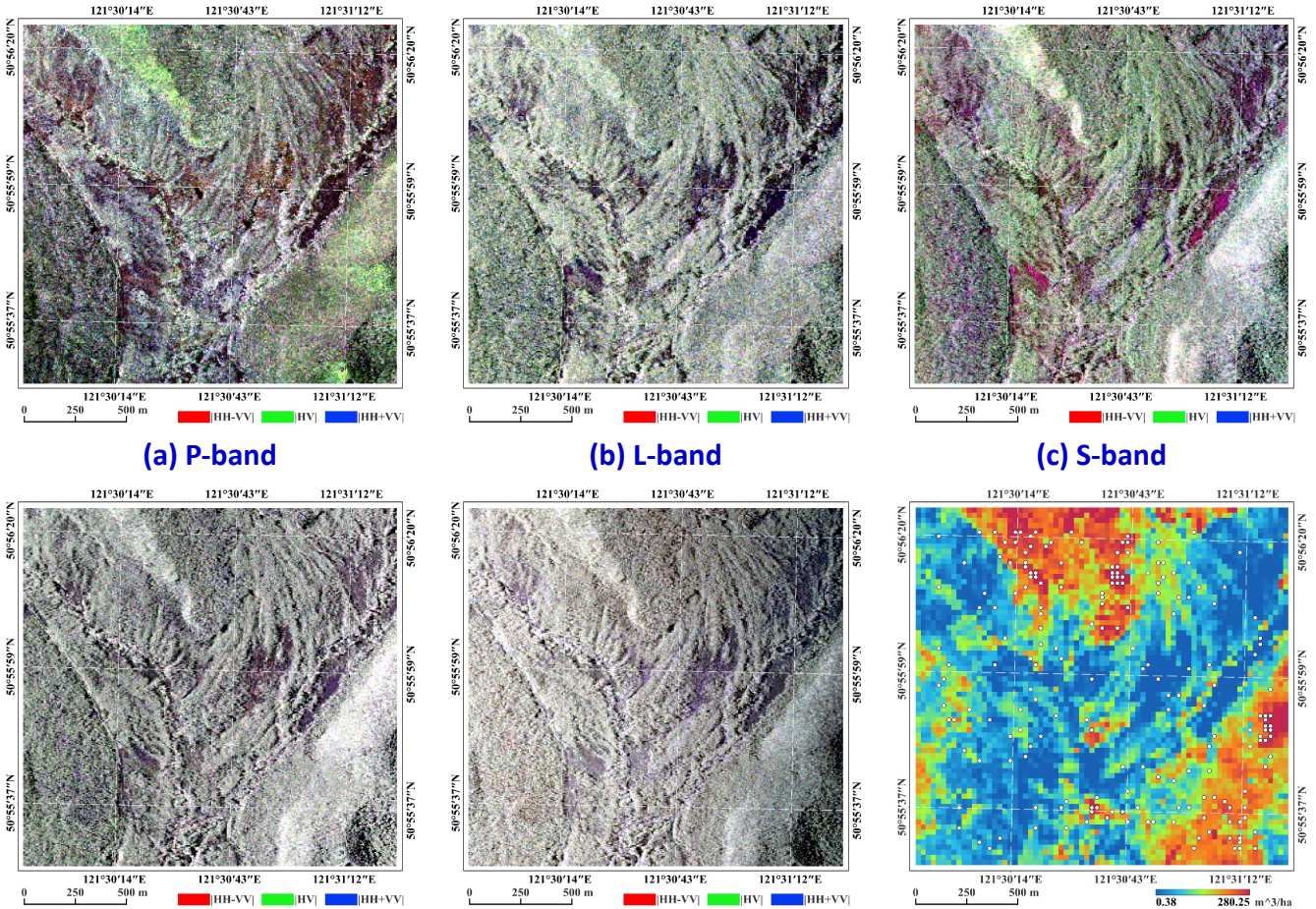

(a) P-band (b) L-band (c) S-band

(d) C-band (e) X-band (f) LiDAR Volume

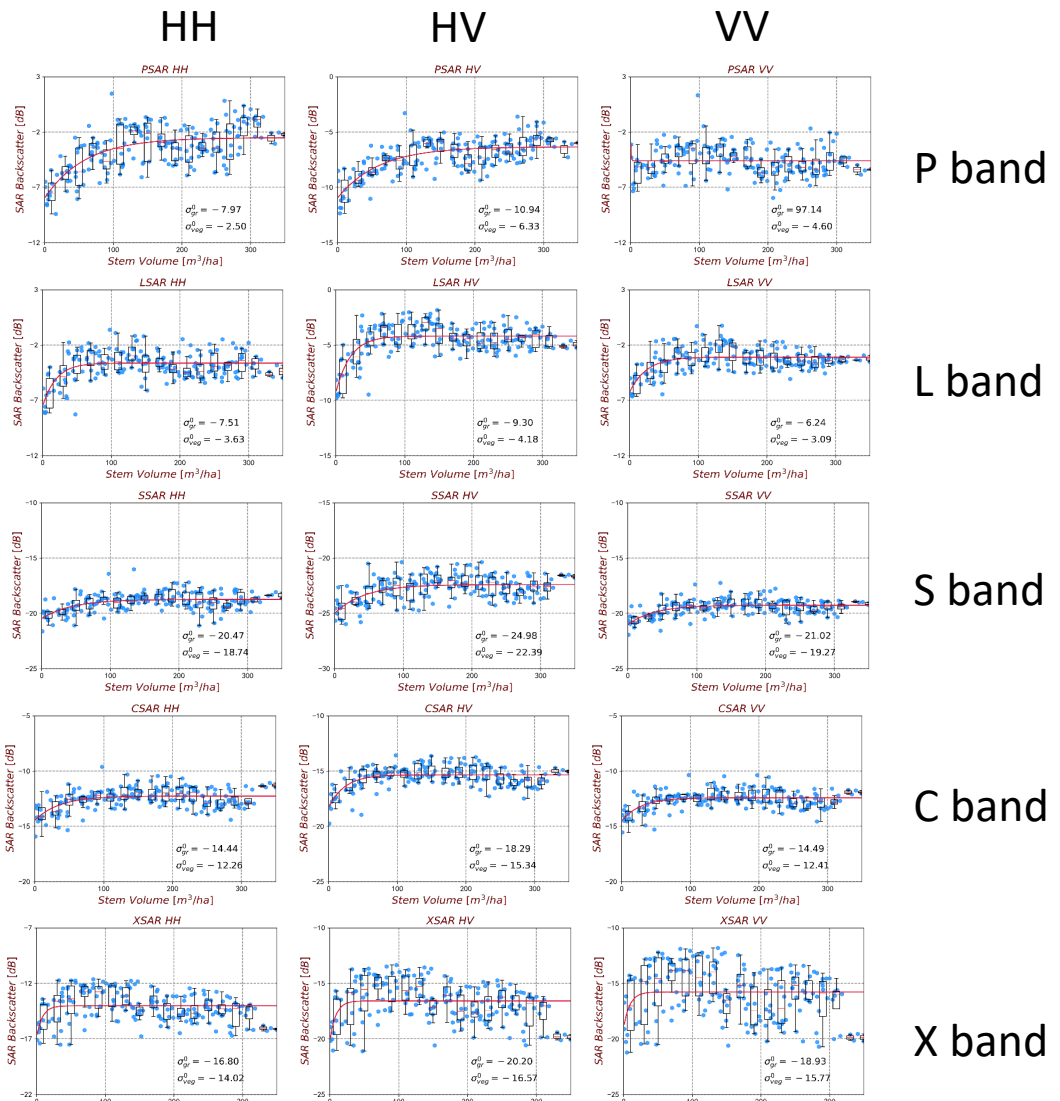

P band

L band

S band

C band

X band

4.1 Assessment of High-resolution Airborne Multi-band PolSAR to Estimate Forest Stem Volume

■ Performance evaluation results

- **Stem volume estimation for single-frequency**

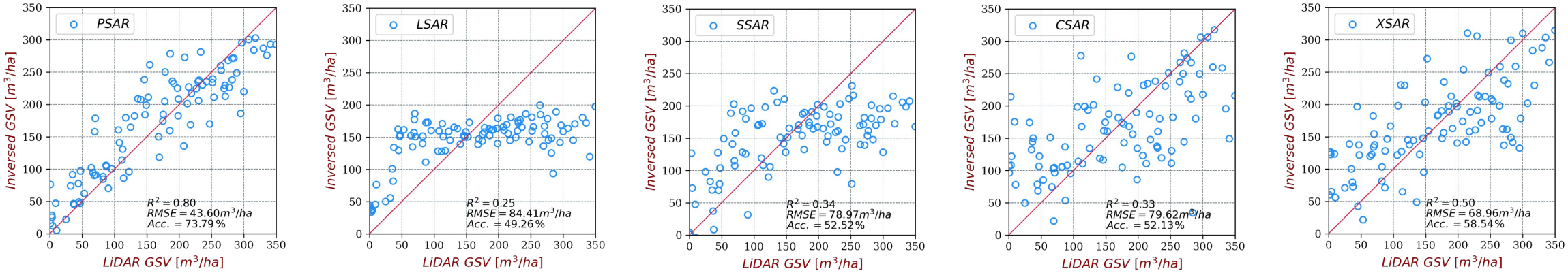

- **Complementarity of L, S, C and X with P-band**

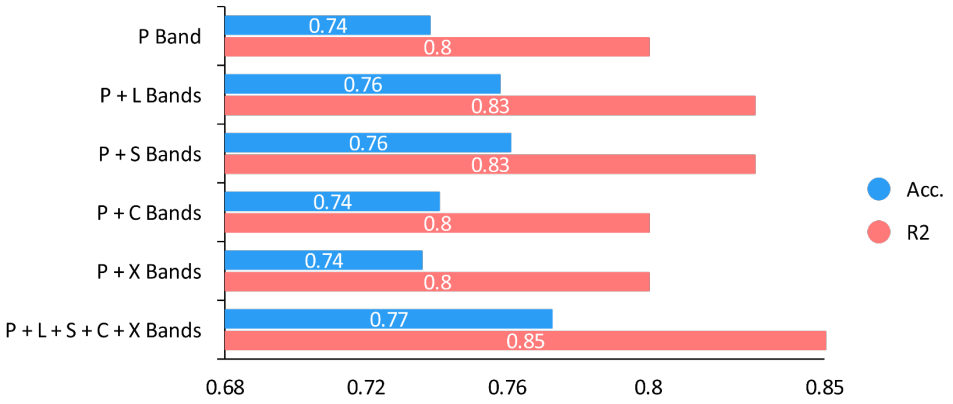

- **Key conclusions**

(1) P band is the first choice for estimation of forest stem volume using PolSAR data.

(2) When using multi-frequency joint estimation, the combination of P and L or S bands should be preferred.

4.2 Forest height & AGB estimation from X- & P-band InSAR data

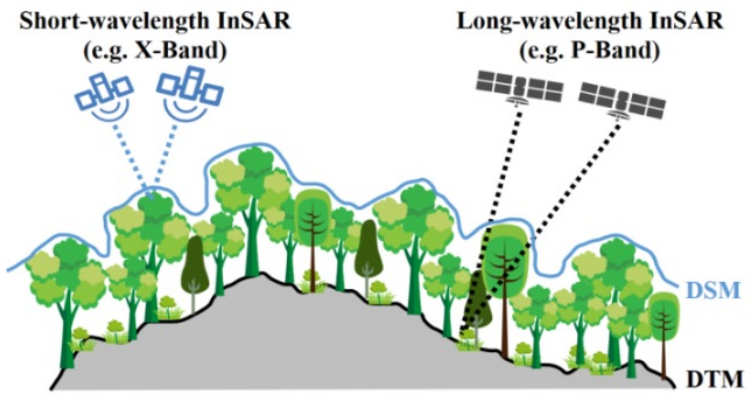

Under-estimate DSM Over-estimate DTM

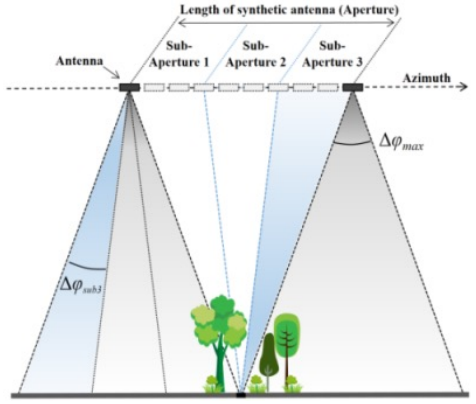

Sub-aperture decomposition to get the true ground surface phase

(Fu, H. et al, remote sensing,2017)

Acc.=86.6%
RMSE=1.8m

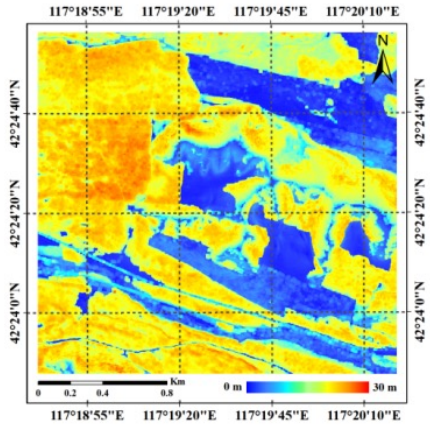

LiDAR H100

validation

DSM bias MLM

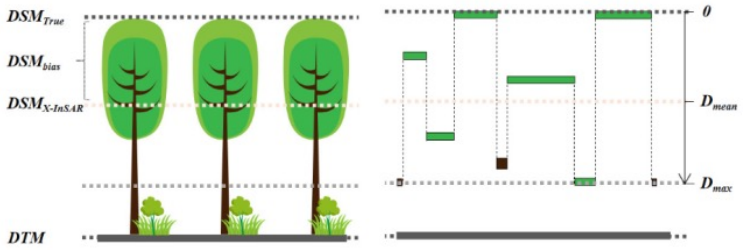

$$f(x) = \frac{1}{D_{max}}, x \in (0, D_{max})$$

$$DSM_{\text{bias}} = \text{Dmax}/2 = \frac{\pi}{|k_z|}\left(1 - \frac{2}{\pi}\sin^{-1}\left[|\gamma|^{0.8}\right]\right)$$

(Xu K., Zhao L., et al, remote sensing,2022)

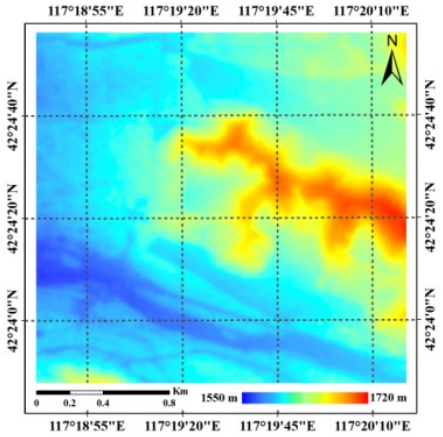

DSM after bias compensation

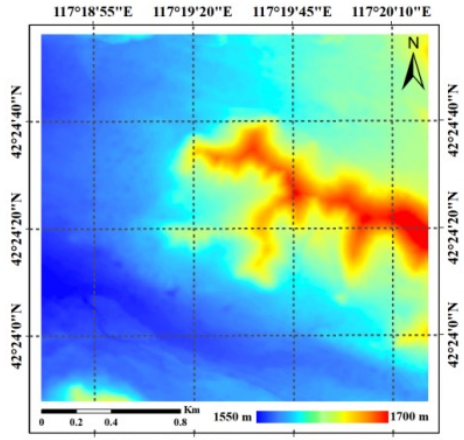

DTM derived from sub-aperture

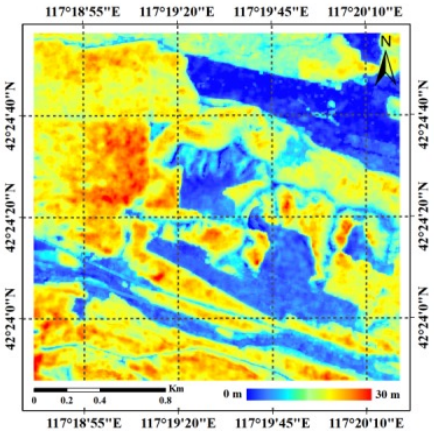

Forest height

4.2 Forest height & AGB estimation from X- & P-band InSAR data

Methods

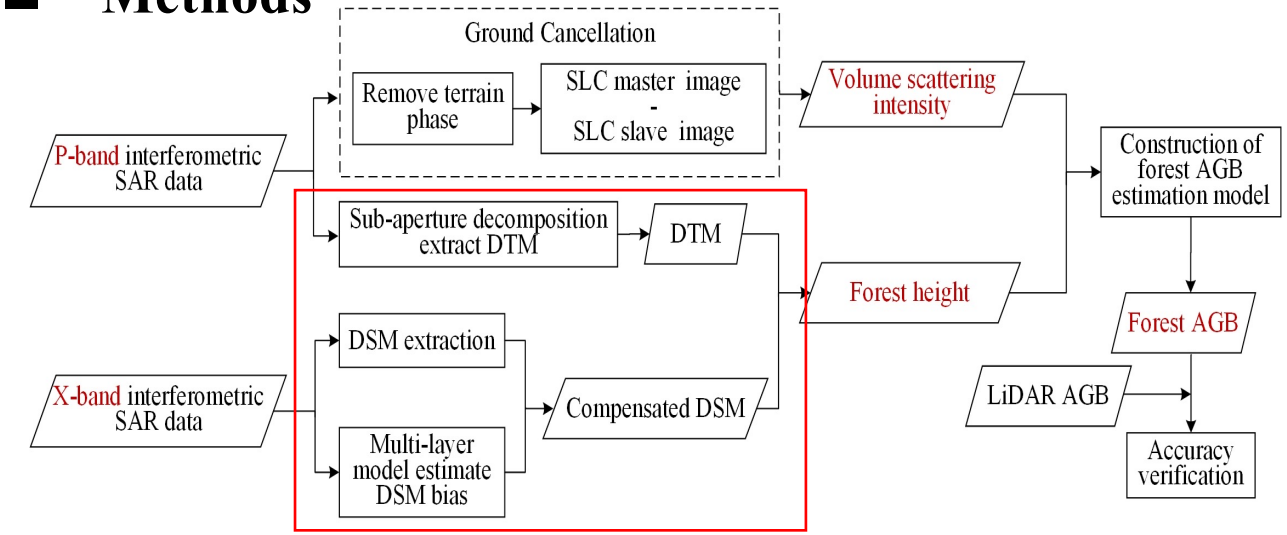

Test site(Saihanba Forest Farm)

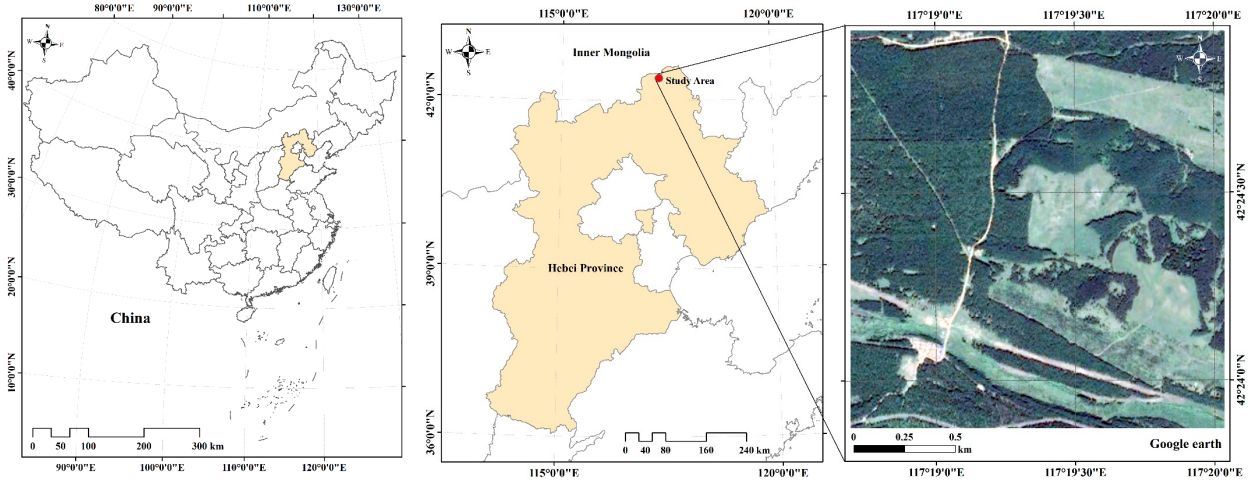

Data

P-band InSAR data (Airborne SAR system, 2019.10.29)

X-band InSAR data (TanDEM-X system, 2018.12.29)

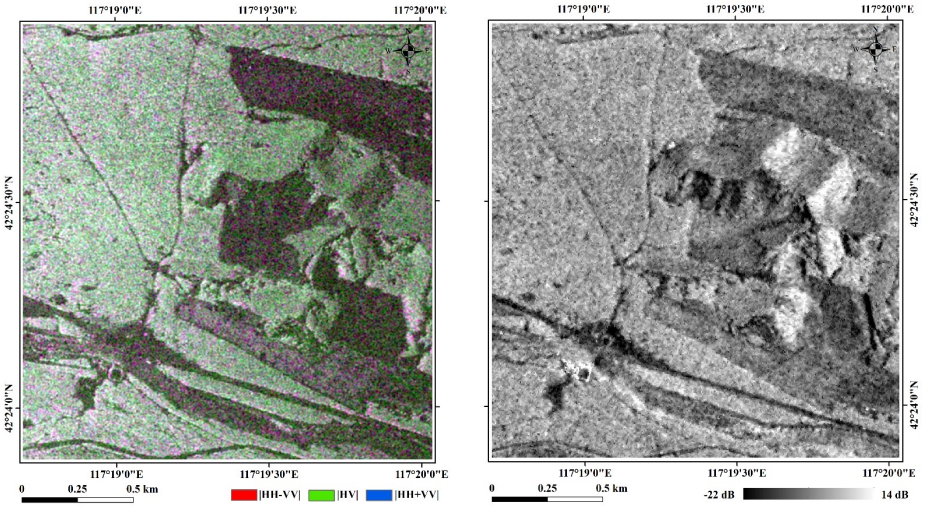

Pauli RGB image of the P-band master image

X-band master image backscatter intensity image

4.2 Forest height & AGB estimation from X- & P-band InSAR data

■ Results

Forest height extraction results

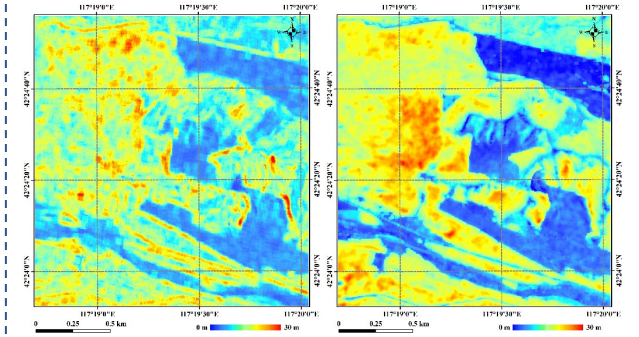

X-band X+P band

Backscatter intensity & AGB

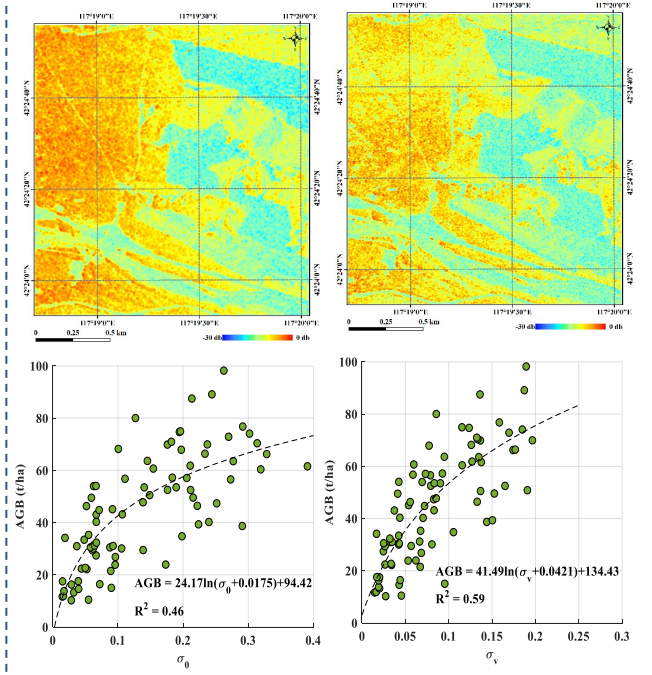

Total backscatter volume backscatter

AGB estimate the results

P-band volume backscatter P+X band fore st height

Acc.=72.60%
RMSE=12.7 t

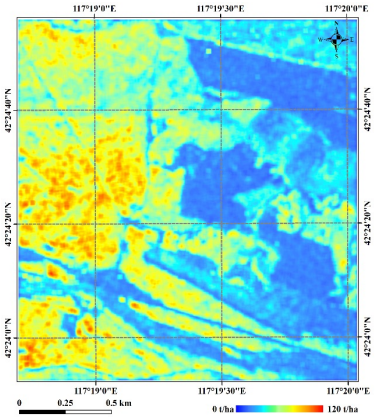

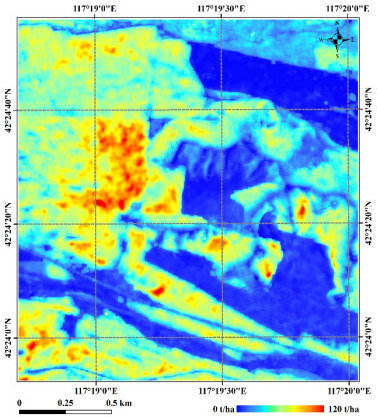

Acc.=80.12%
RMAE=9.21 t

Acc.=83.73%
RMSE=7.54 t

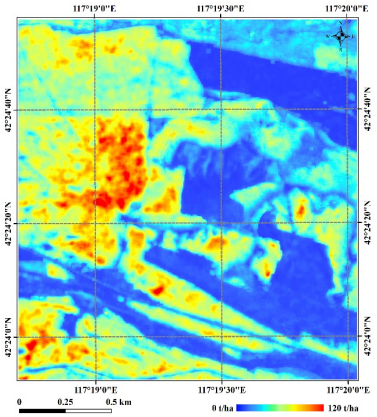

P+X band forest height and volume backscatter

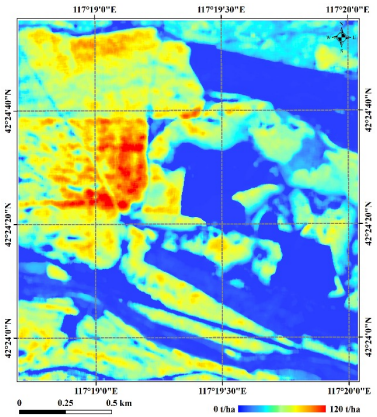

LiDAR AGB

4.3 A new approach of phase calibration for TomoSAR over forested area

■ **A new approach combining polynomial fitting (PF) and entropy minimization (EM)**

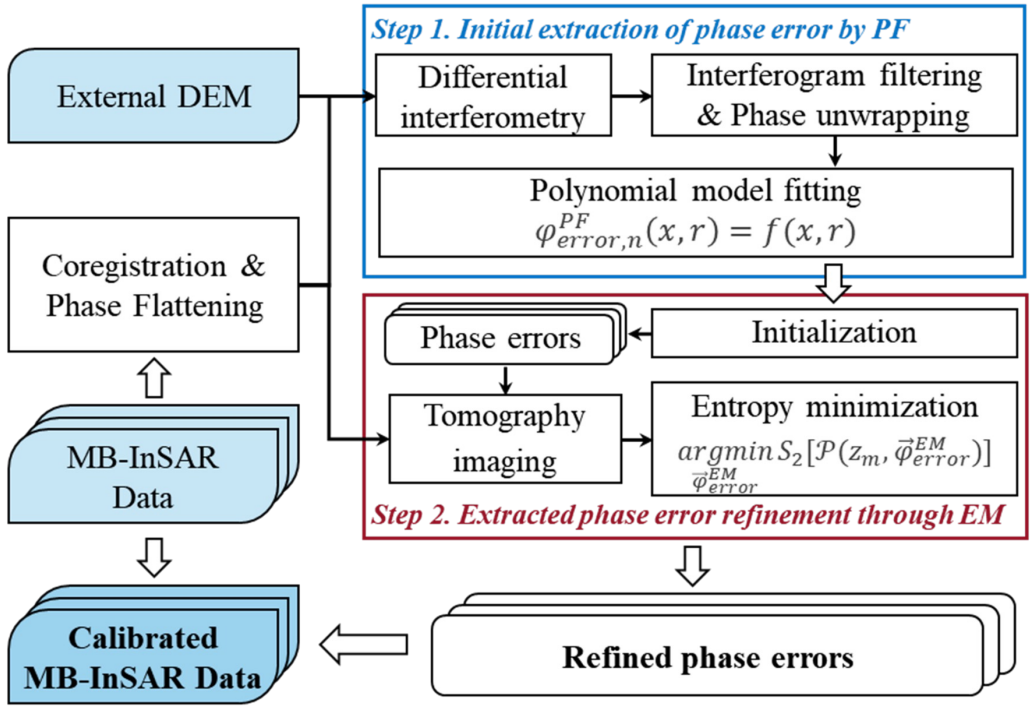

- **Step 1: Initial extraction of phase error by PF**
  - ✓ **Modeling the dominant part of the phase error.**
- **Step 2: Extracted phase error refinement through EM**
  - ✓ **Estimating the residual phase error.**

Residual phase errors before and after calibration

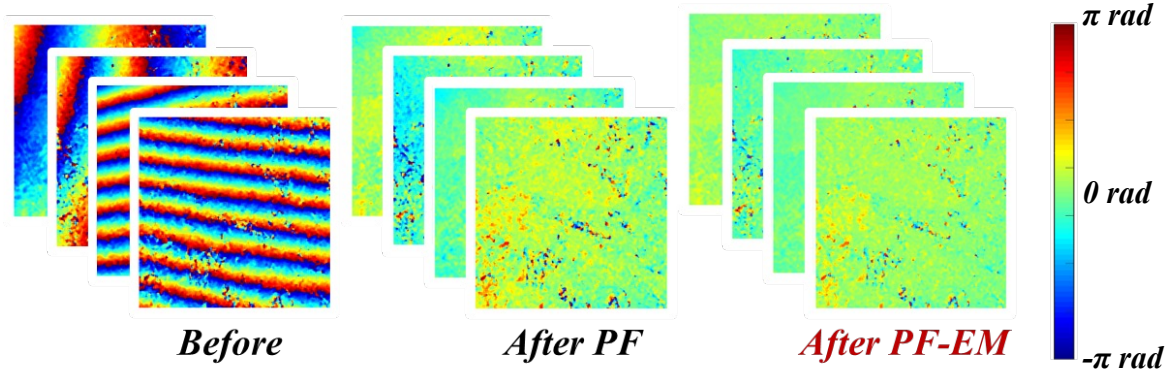

Tomography profile before and after calibration

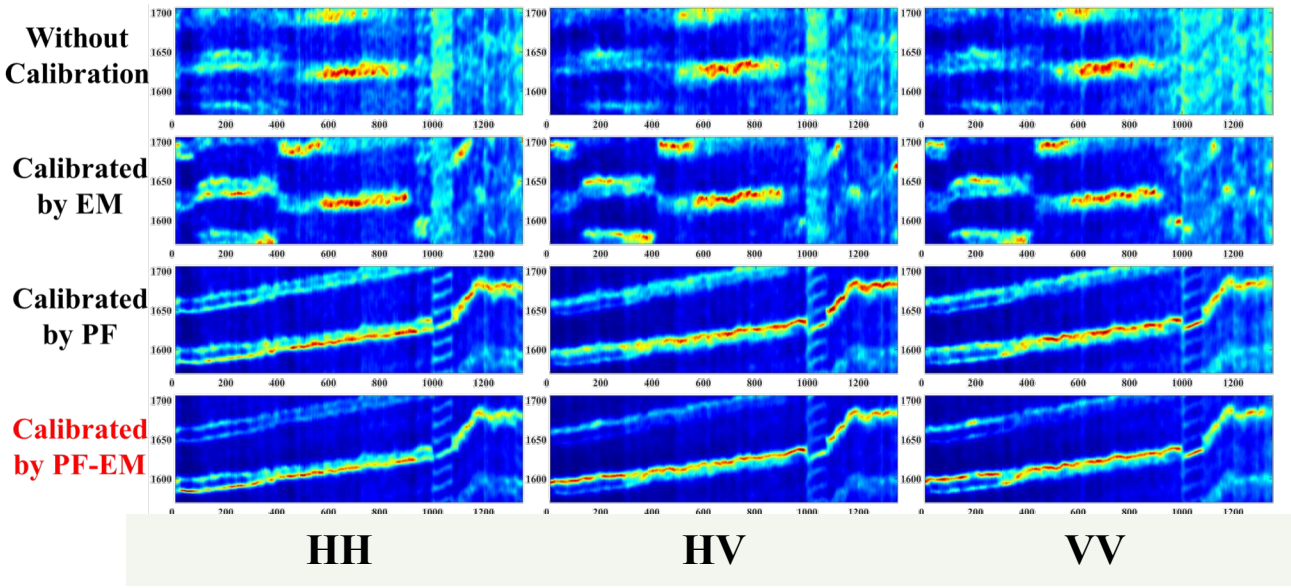

4.3 A new approach of phase calibration for TomoSAR over forested area

- **TomoSAR forest height extraction result based on proposed method**

Test site: Saihanba Forest Farm

Data: P-band MB-InSAR data (6 tracks)

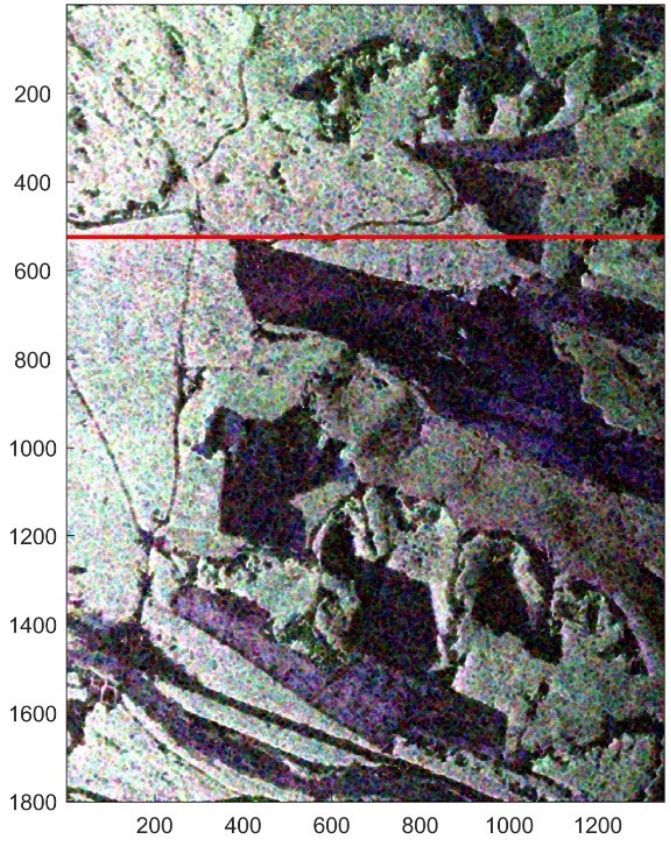

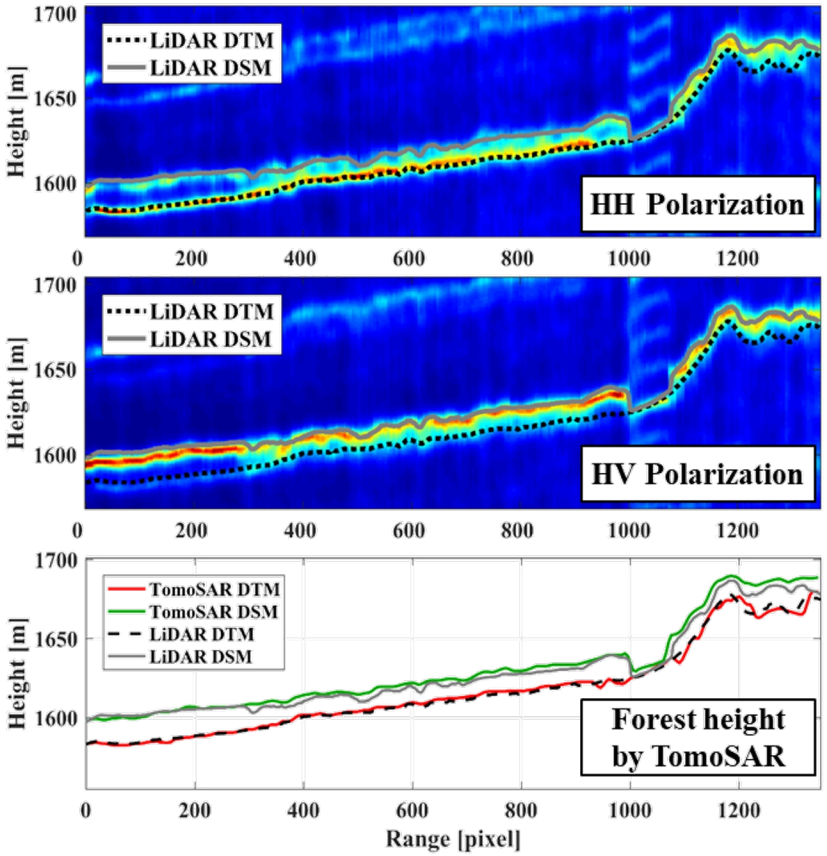

LiDAR CHM

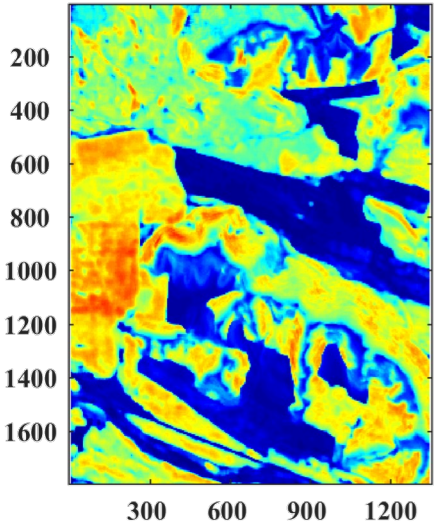

TomoSAR forest height

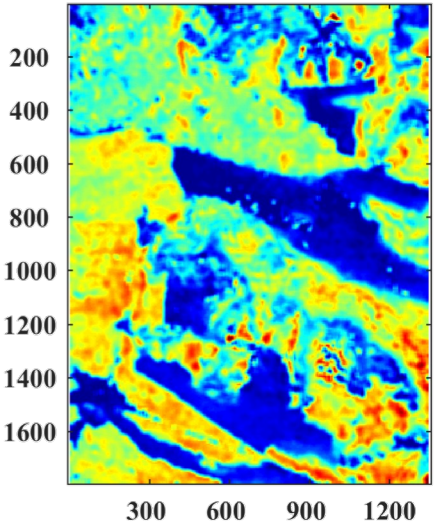

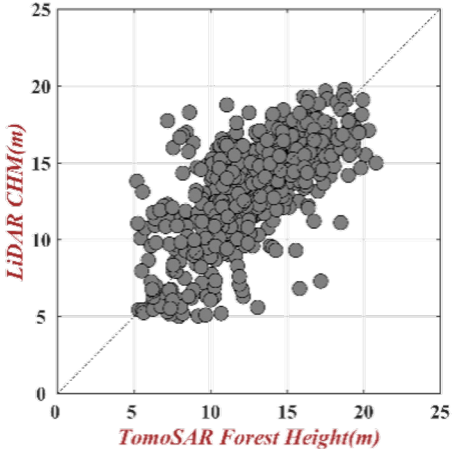

RMSE=2.61 m

Acc.=80.52%

R^2=0.45

4.3 A new approach of phase calibration for TomoSAR over forested area

Test site: Genhe Forest Farm

Data: P-band MB-InSAR data (10 tracks)

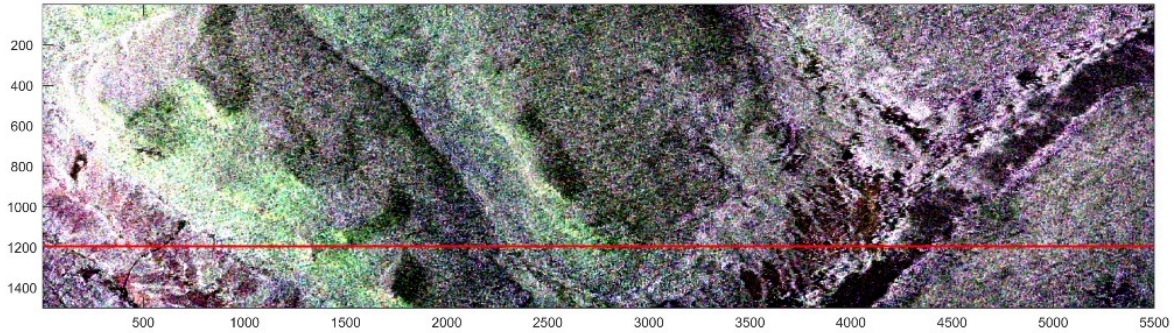

HH polarization tomography profile

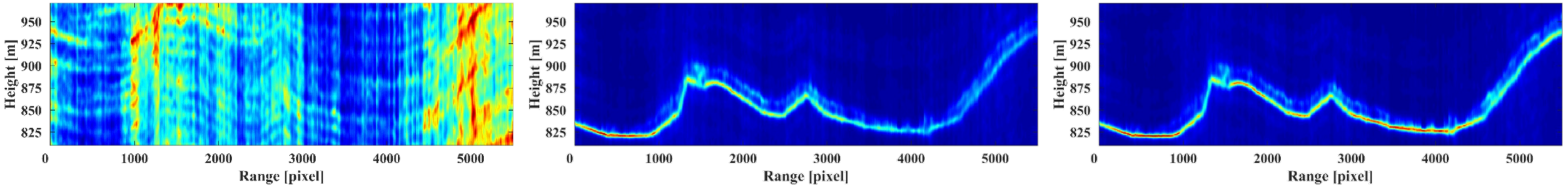

Pauli RGB Display of tomography profile

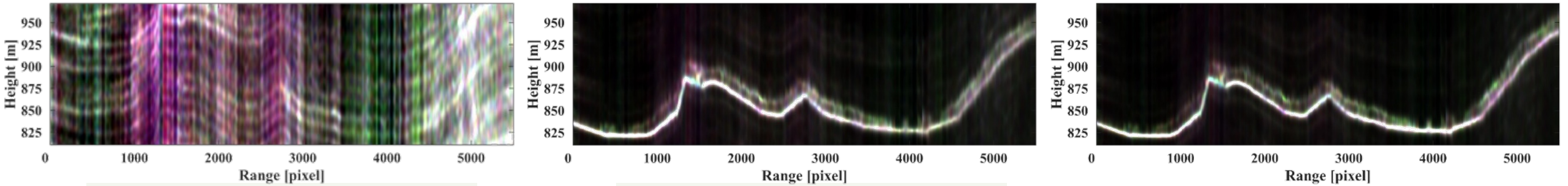

Without calibration | Tradition method | Proposed method

4.4 TomoSAR—Forest underlying topography estimation

- **Dual polarimetric TomoSAR (DP-TomoSAR) is proposed as a suitable candidate to estimate forest underlying topography because of its wide swath and multiple polarimetric observations.**

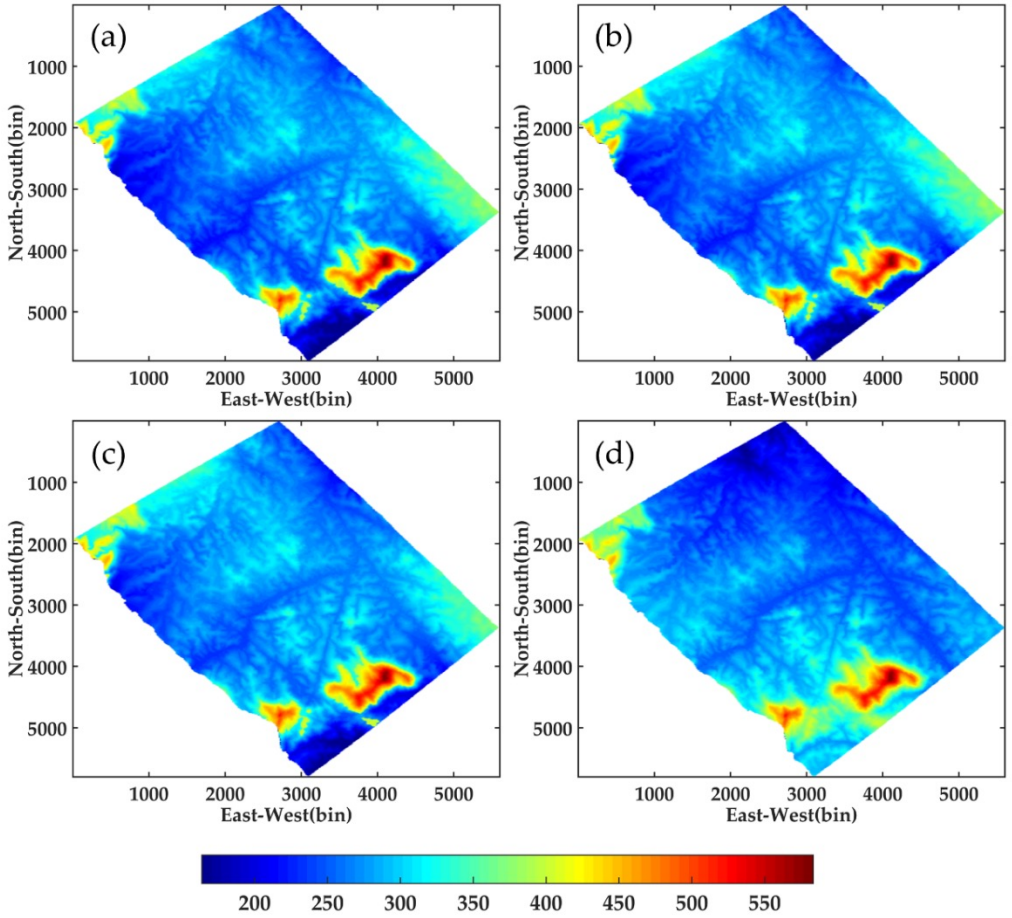

Underlying topography: (a) DP-Beamforming (b) DP-Capon (c) DP-MUSIC and (d) LiDAR

RMSE of underlying topography estimated by different algorithms using SP-TomoSAR, DP-TomoSAR and FP-TomoSAR.

Method	Data Type	RMSE (m)
Beamforming	SP	9.24
	DP	8.25
	FP	8.07
Capon	SP	9.20
	DP	8.09
	FP	7.92
MUSIC	SP	9.18
	DP	8.17
	FP	8.01

The underlying topography obtained by different DP-TomoSAR algorithms maintain a high consistency in texture features. The accuracy of the results retrieved by all the three algorithms using DP-TomoSAR and FP-TomoSAR is close, and both of them are superior to those of SP-TomoSAR.

Xing Peng, Youjun Wang, Shilin Long, Xiong Pan, Jianjun Zhu, Xinwu Li. Underlying Topography Inversion Using TomoSAR Based on Non-Local Means for an L-Band Airborne Dataset. Remote Sensing, 2021, 13(15), 2926.

4.4 TomoSAR—Forest underlying topography estimation

- **Nonlocal means(NLM) TomoSAR** on ESA BioSAR 2008 datasets

	Beamforming	Capon	MUSIC
LM	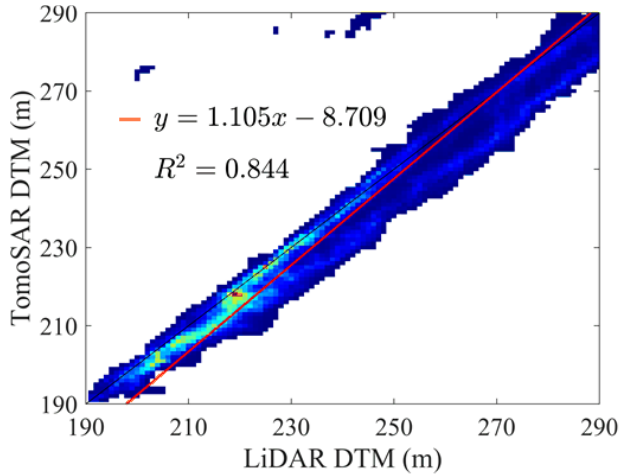	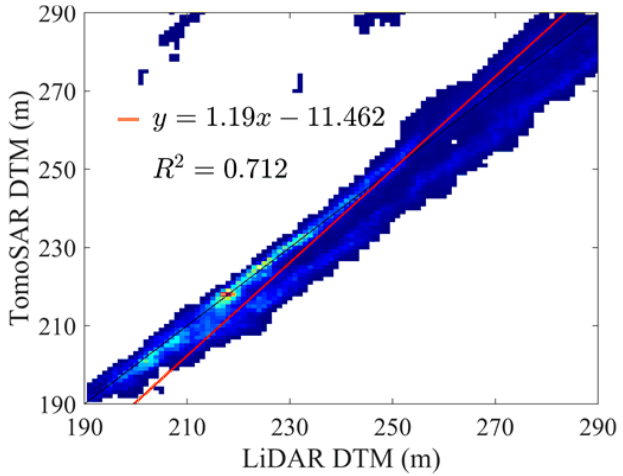	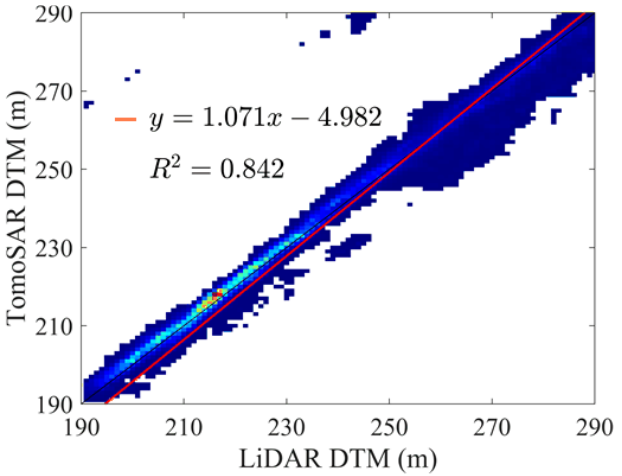
	(a)	(b)	(c)
NLM	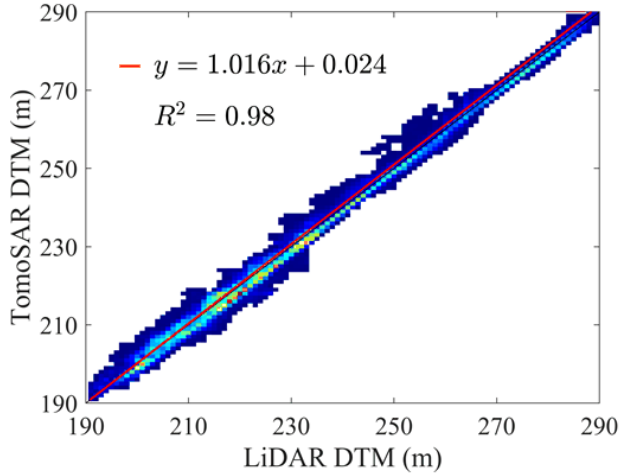	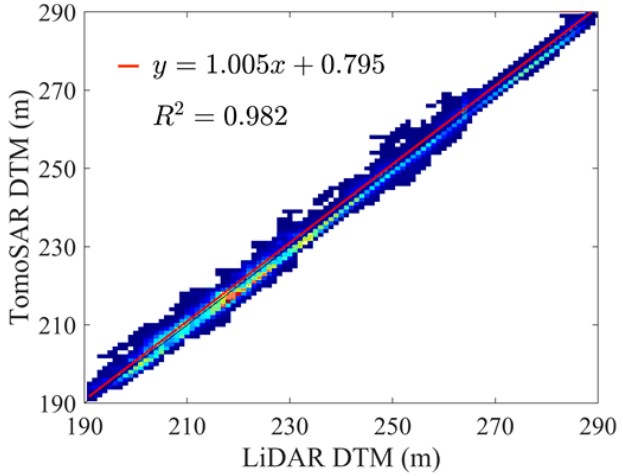	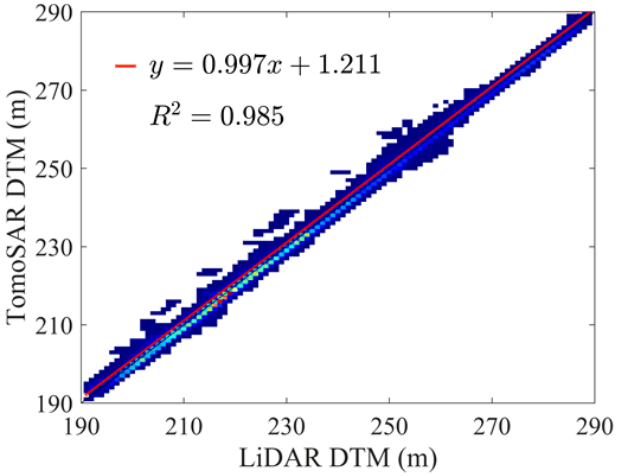
	(d)	(e)	(f)

4.5 TomoSAR——Building height estimation

- **TomoSAR reconstruction algorithm based on CS Atomic Norm Minimization (Tomo-ANM)**
  - **ANM is a continuous compressed sensing technique, and its fast realization, IVDST, is utilized to accelerate the process.**
  - **SL1MMER is shown as a reference.**

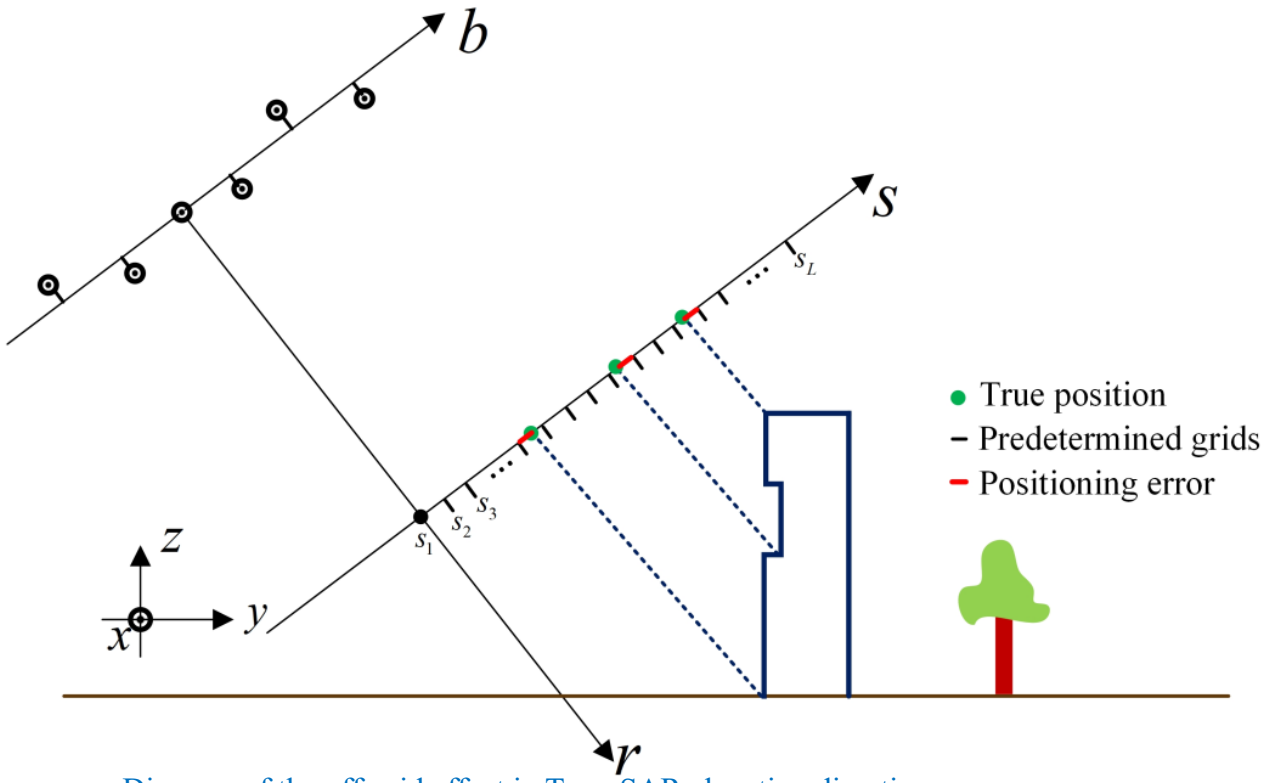

Diagram of the off-grid effect in TomoSAR elevation direction.

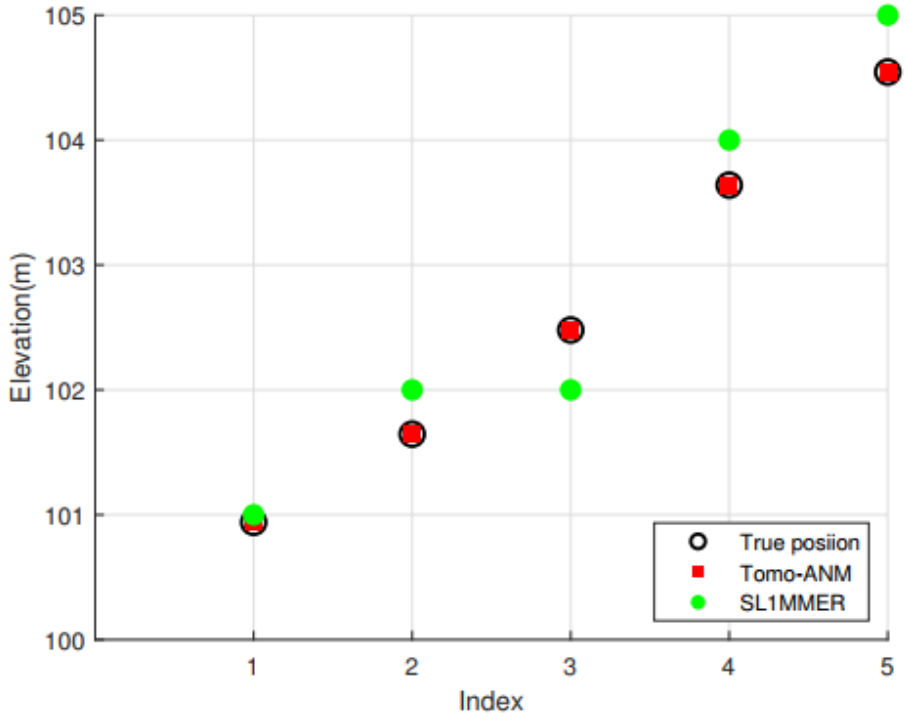

Removal of the off-grid effect by Tomo-ANM.

4.5 TomoSAR——Building height estimation

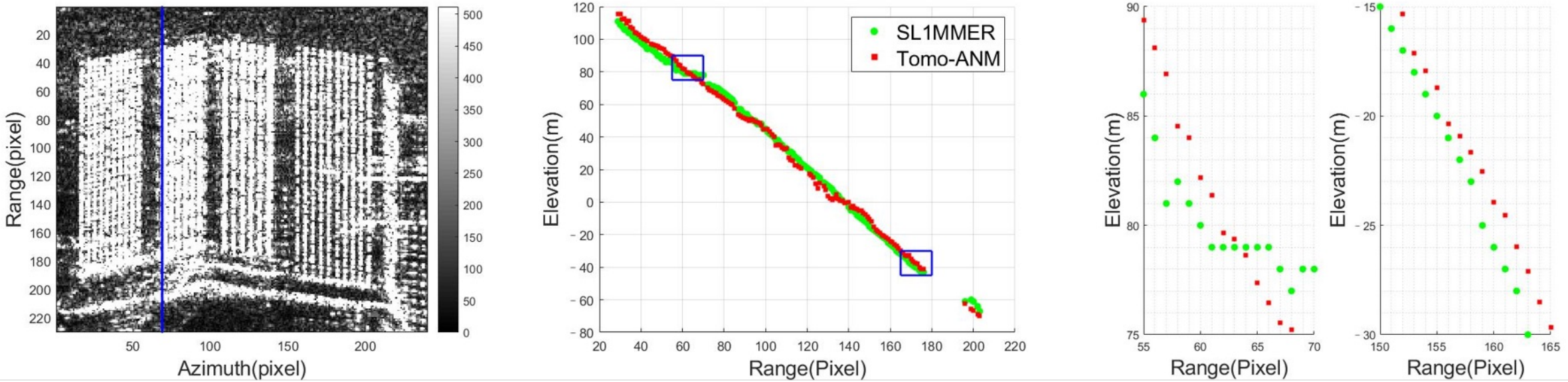

Real data results: (a) SAR image. Blue line is used to show tomographic profiles . (b) The Tomo-ANM and SL1MMER profiles of line azimuth 69. (c) Partial enlargement of the blue rectangle in (b).

Height estimation of different methods. The true height of the building is 99 m.

	Building Height(m)	Estimation Error(m)
Tomo-ANM-CVX	**96.62**	2.40%
Tomo-ANM-IVDST	**95.70**	3.33%
SL1MMER	91.84	7.23%

We used eight stacks TerraSAR staring spotlight data to conduct real data experiments. The results showed that, compared with the on-grid algorithm, Tomo-ANM can eliminate the off-grid effect, so as to better position scatterers and obtain more accurate building height estimation results.

Ning Liu, Xinwu Li, Xing Peng, Wen Hong, SAR Tomography Based on Atomic Norm Minimization in Urban Areas. *Remote Sensing.* **2022**, *14*, 3439.

4.6 Preparation of ESA's BIOMASS mission ——Insights of TowerScat campaigns

Côté Ouest de la tour

Réseau des 20 antennes bandes P+L

6 antennes bande C

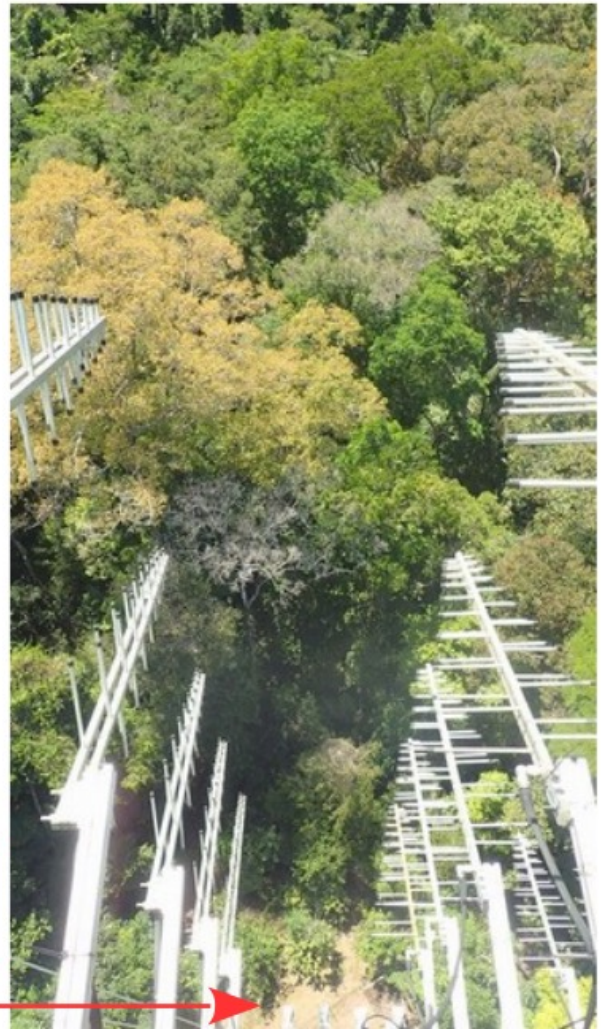

Côté Nord-Est de la tour

2 antennes large bande (6-18GHz)

6 antennes bande C

Tropiscatm Paracou, French Guyana

4.6 Preparation of ESA's BIOMASS mission ——Insights of TowerScat campaigns

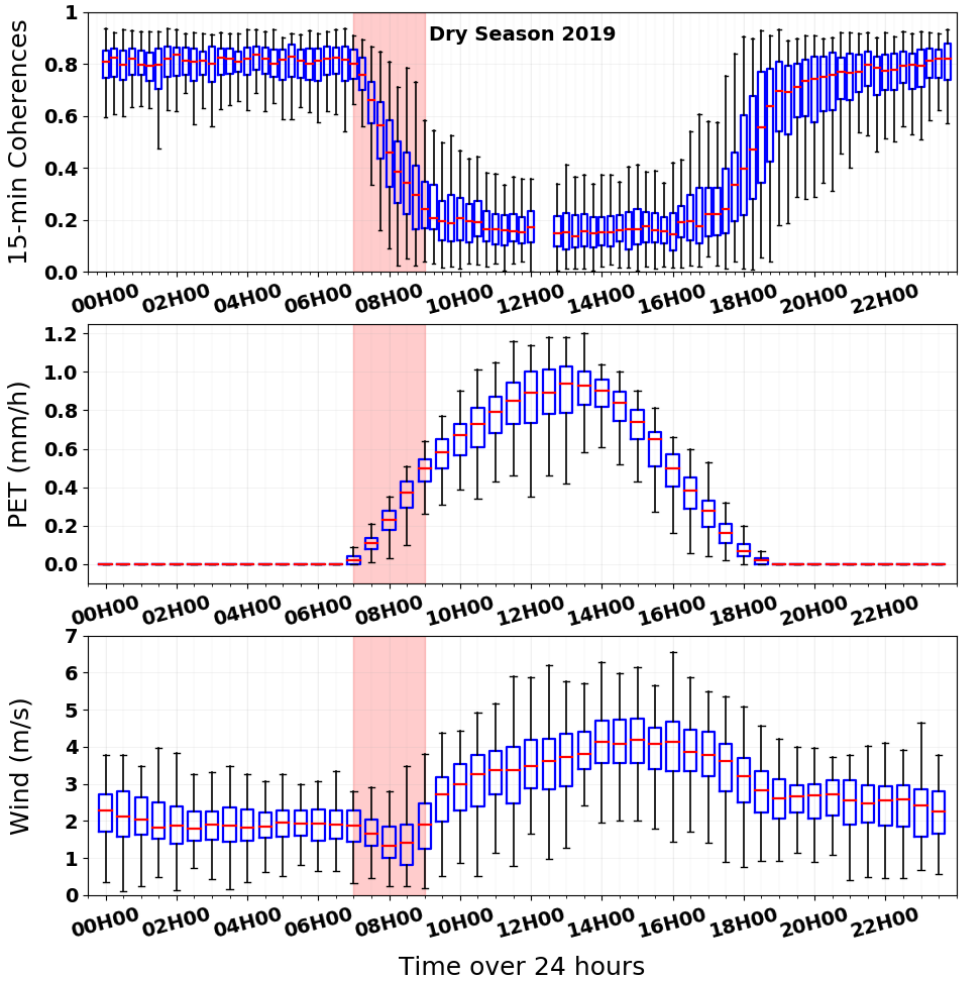

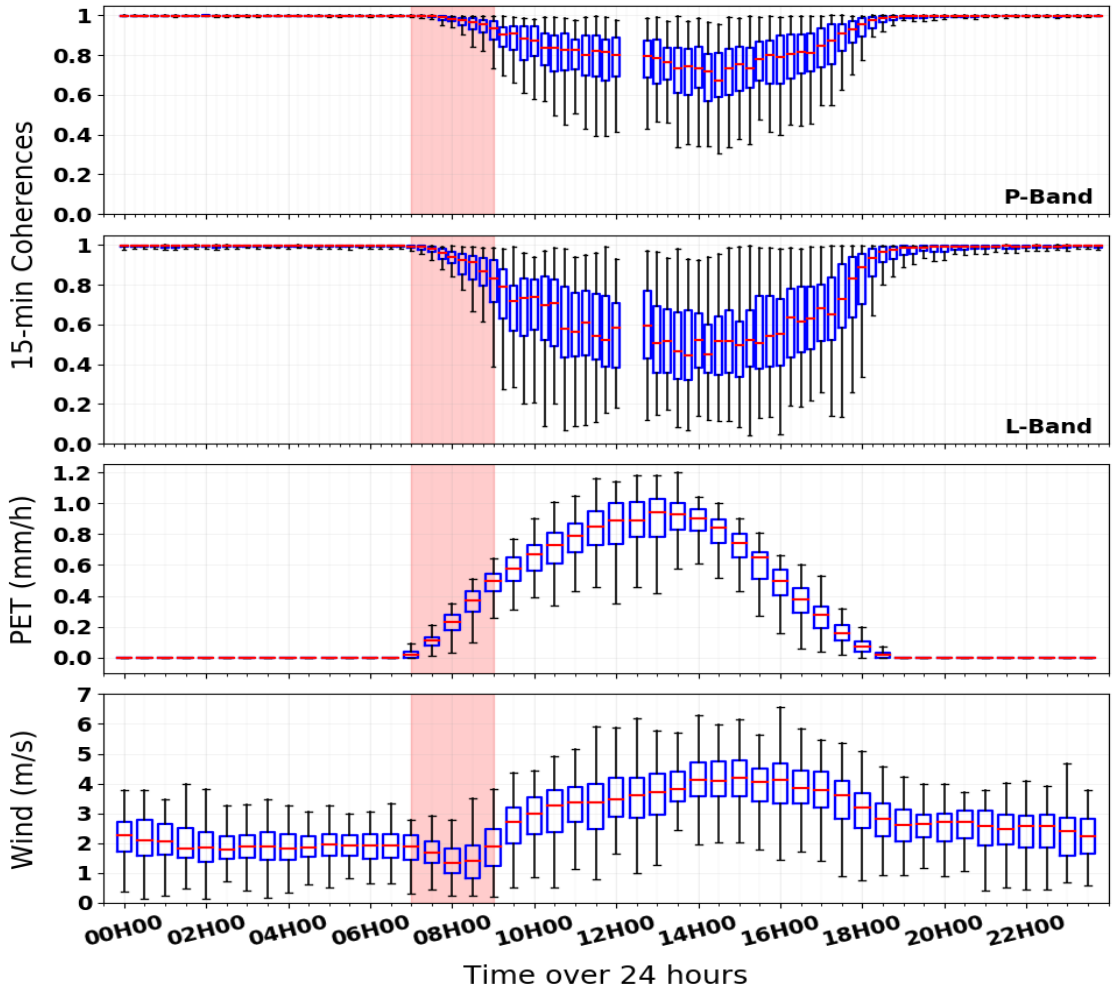

C-band 15min-decorrelation patterns can be explained by evapotranspiration, not wind speed

Evapotranspiration plays a key role at L an P bands too

El Idrissi Essebtey, Villard 2021, 2022

4.6 Preparation of ESA's BIOMASS mission ——BIOMASS programmatic sequence

BIOMASS mission sequence of operating modes

Tomographic Phase:
7 x 3-day repeat
15 months for global coverage

Interferometric Phase:
3 x 3-day repeat; 7 months for global coverage
≈ 4 years time series

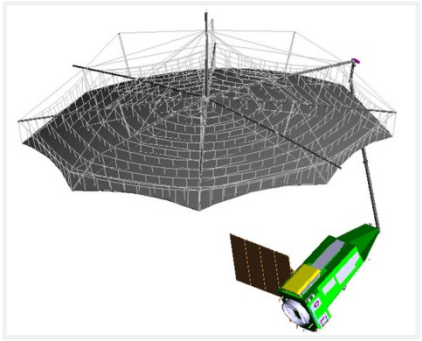

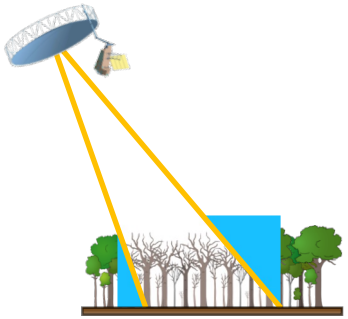

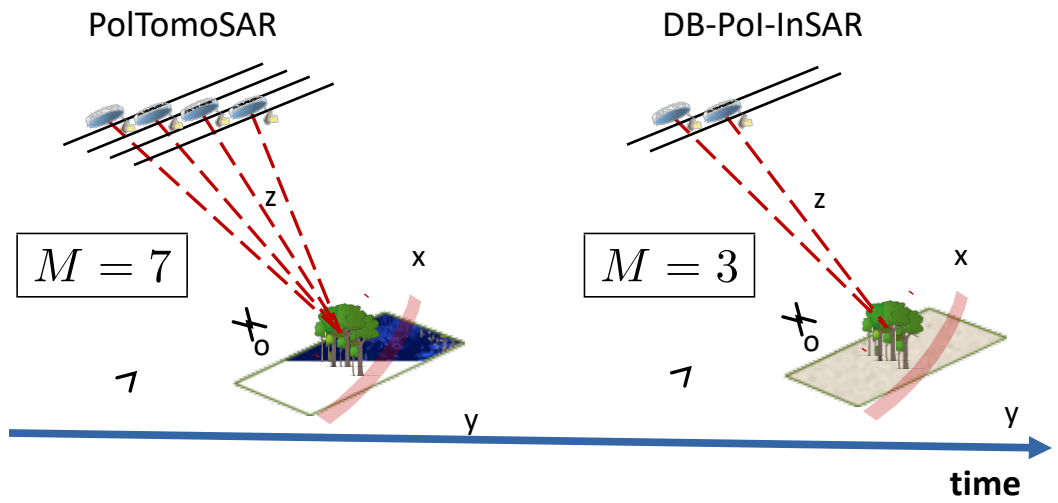

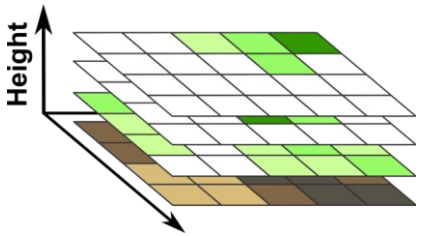

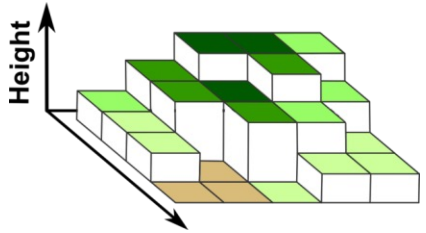

→ **Synergistic use of priors**

→ **Performance quantification**

4.6 Preparation of ESA's BIOMASS mission ——Use of auxiliary priors

Standard deviation of tree height estimates

σ_{h_v}

$10\,m$

$0\,m$

PolTomoSAR

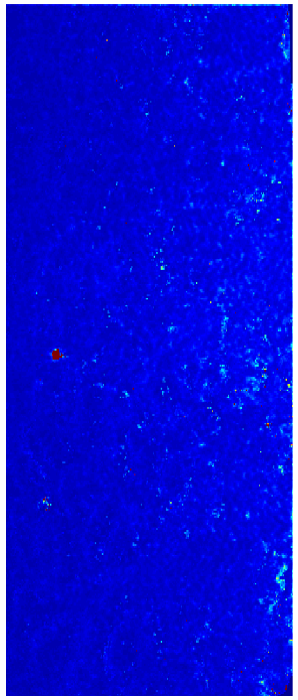

$M = 6, N_p = 3$

SP TomoSAR

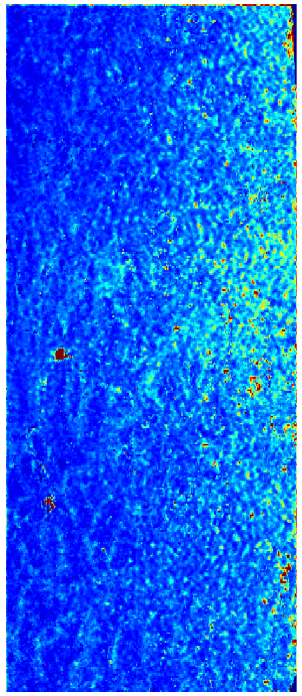

$M = 6, N_p = 1$

DB PolinSAR

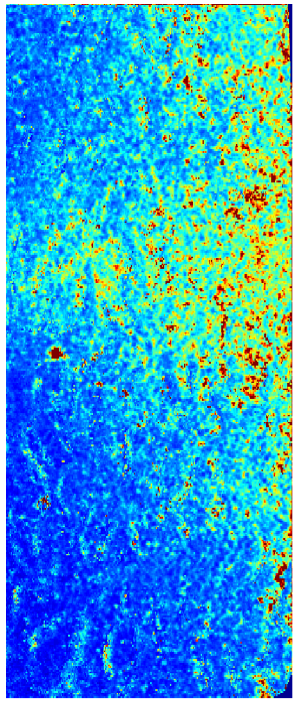

$M = 3, N_p = 3$

DB vert. resolution

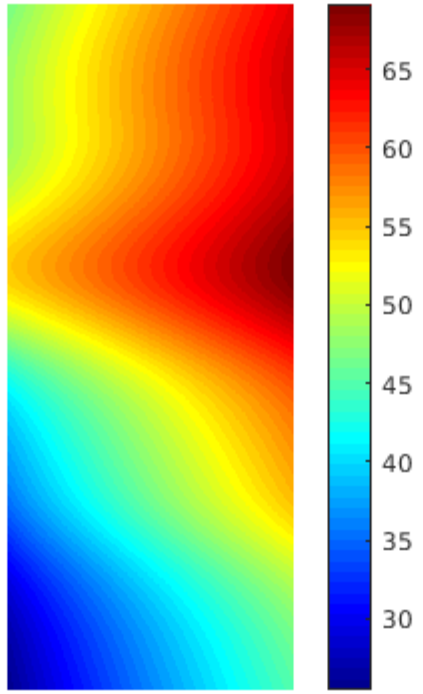

$\delta z[m], M = 3$

DB PolinSAR **+ PolTomo Ke prior**

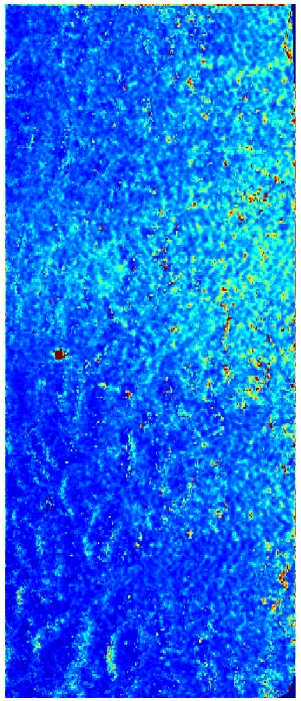

- **Absolute variability values depend on processing configuration**
- **Sensitivity to vertical resolution**
- **Auxiliary information (priors)→overcome resolution related issues**

4.7 A Temporal Polarization SAR Classification Method Based on Polarimetric-Temporal Feature Selection

Method

Overall network structure

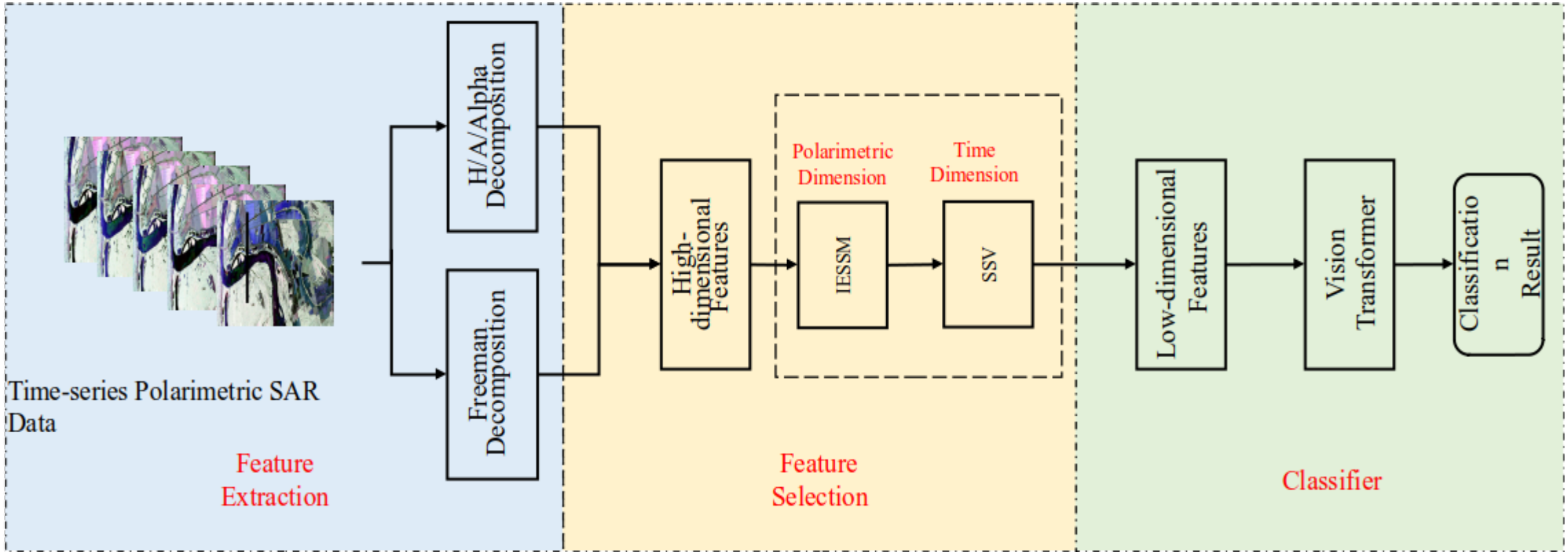

Polarization decomposition of the pre-processed time-series polarimetric SAR image

For the decomposed high-dimensional features, feature selection is performed from polarization and time dimensions.

Verification of feature selection results by Vision Transformer

Beijing University of Chemical Technology (BUCT), Q. Yin

Experiment and conclusions

This paper uses the data of UAVSAR for experiments. It includes 5 Fully-PolSAR images from July 1, 2019 to September 23, 2019. It contains 16 categories, and the labeling area has a total of 9047044 pixels.

2019-07-01

2019-07-16

2019-07-25

2019-08-12

2019-09-23

Ground Truth

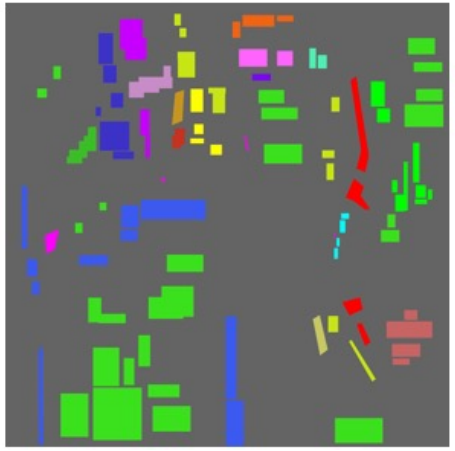

4.7 A Temporal Polarization SAR Classification Method Based on Polarimetric-Temporal Feature Selection

Experiment and conclusions

Features	IESSM	SSV	IESSM+SSV
Alpha	0.8995	0.2661	**1.1656**
Anisotropy	0.9171	0.5520	1.4691
Beta	0.9077	0.4850	**1.3927**
(1-H)(1-A)	0.8563	0.3491	**1.2054**
(1-H)A	0.7893	0.4473	**1.2312**
H(1-A)	0.8961	0.4971	**1.3932**
HA	0.9223	0.4925	1.4148
Delta	0.9137	0.5090	1.4227
Entropy	0.8532	0.3510	**1.2042**
Gamma	0.9176	0.7269	1.6445
Lambda	0.9084	0.2603	**1.1687**
Freeman_Dbl	0.8730	0.3831	**1.2561**
Freeman_Odd	0.8642	0.5951	1.4593
Freeman_Vol	0.8922	0.2275	**1.1197**

Method	Accuracy
ResNet-14+all 14 features	86.68%
Vision Transformer +all 14 features	**88.02%**
ResNet-14+9 features	85.99%
Vision Transformer +9 features	**87.38%**

- 9 features were selected by the proposed feature selection method
- It achieves equal accuracy compared to all features.

*Zhiyuan Lin, Jiaxin Cui, Qiang Yin et.al. Time-series PolSAR crop Classification based on joint feature extraction (IGARSS2022(EI),Oral)

4.8 Multi-Temporal PolSAR Classification Based on Time-Variant Scattering Features from T matrix operation in time dimension

Multi-Temporal Polarimetric SAR data

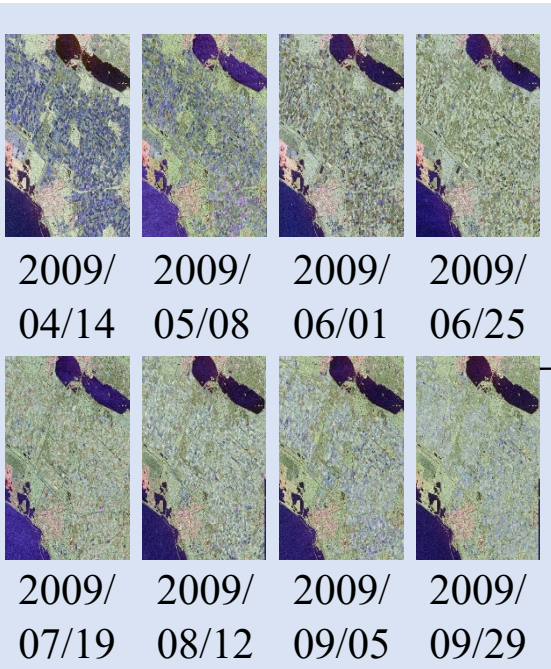

Radarsat-2 data

Data Model Representation

Multiplication Model
$T_M = T_{t1}^{-1} T_{t2}$

Difference Model
$T_D = T_{t1} - rT_{t2}$

Traditional Model
$T_{t1}, T_{t2}, T_{ti}, T_{tj} \ldots T_{tn}$

Time-variant Scattering Features Extraction

Eigenvalues
Target Randomness(p_R)
Polarization Fraction(PF)
Polarimetric Asymmetry(PA)
...

Pauli Decomposition
H/A/α Decomposition
Freeman Decomposition
...

H/A/α Decomposition
Freeman Decomposition

Static temporal and polarimetric Features

Deep Learning Classifier

Vision Transformer

Performance Comparison

Classification A

Classification B

Classification C

The multiplication and difference data representation model are applied to characterize multi-temporal PolSAR data.

Based on the models, a new series of time-variant scattering features are extracted, which can provide the information of change type and interpret the variation of time series scattering mechanism.

The vision transformer is used for classification.

4.8 Multi-Temporal PolSAR Classification Based on Time-Variant Scattering Features from T matrix operation in time dimension

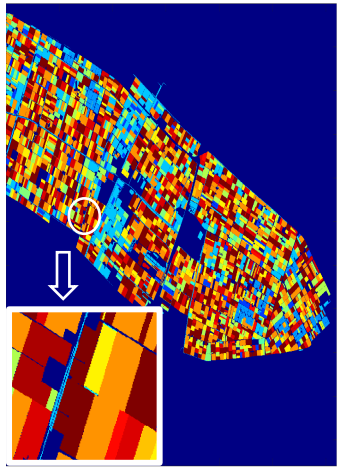

Ground Truth

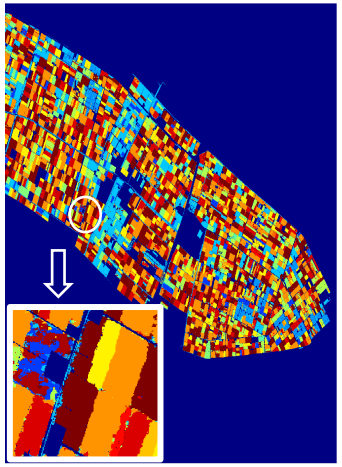

Multiplication Model

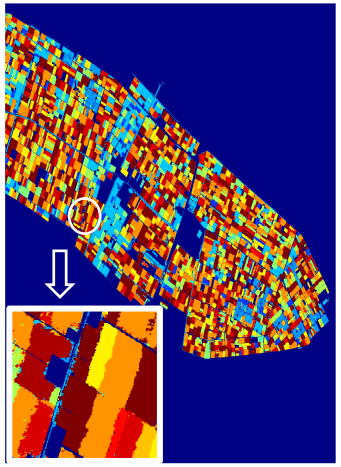

Difference Model

Data Model	Accuracy
Time-variant with Multiplication Model	**87.69%**
Static temporal and polarimetric features	89.23%
Time-variant with Difference Model	**88.96%**
Static temporal and polarimetric features	88.23%

Conclusion

- The Difference model performs better than the Multiplication model.
- The time-variant scattering features have the potential in multi-temporal change analysis.

***Li Gao, Qiang Yin*, Wen Hong.** Classification performance comparison of time variant scattering features of multi-temporal polarimetric SAR data (IGARSS2023 (EI) ,Poster)

4.9 Near-Real Time deforestation monitoring using S1

- 12 days (6 in Europe) time-series → NRT capabilities
- C-band: forest loss detection affected by
  - changing environmental factors (soil moisture...)
  - residual (or regrowing) vegetation

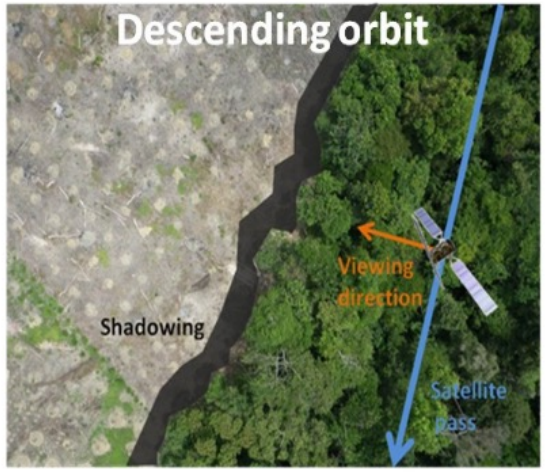

10 May 2015

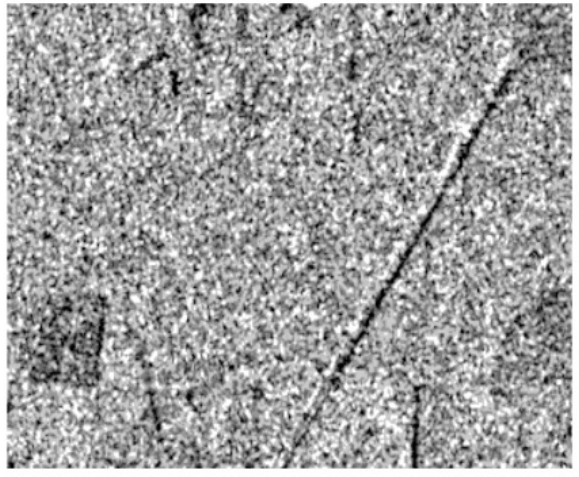

1 October 2016

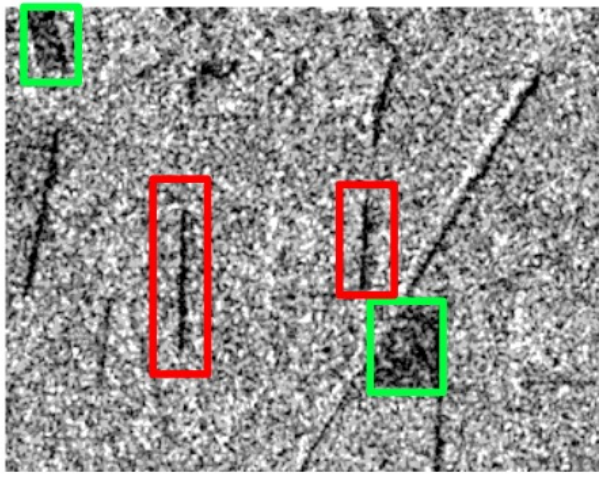

Recent logging
Older logging shadow edge

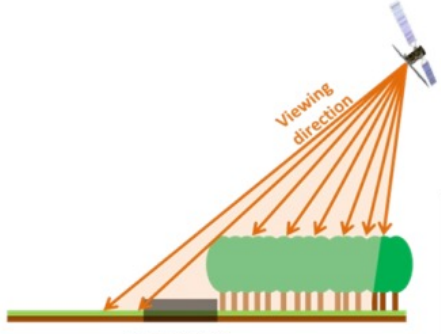

10 m resolution,
>90% accuracy (Peru, Gabon, French Guiana, Brasil and Vietnam)

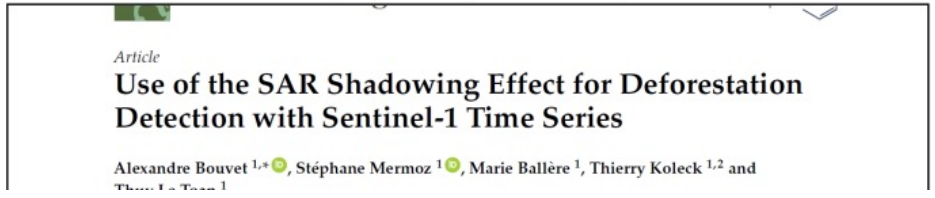

Article

Use of the SAR Shadowing Effect for Deforestation Detection with Sentinel-1 Time Series

Alexandre Bouvet [1,*], Stéphane Mermoz [1], Marie Ballère [1], Thierry Koleck [1,2] and

CESBIO

4.9 Near-Real Time deforestation monitoring using S1

- 12 days (6 in Europe) time-series → NRT capabilities
- C-band: forest loss detection affected by
  - changing environmental factors (soil moisture...)
  - residual (or regrowing) vegetation

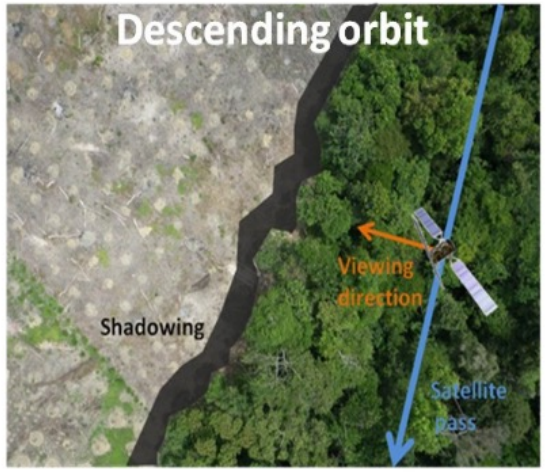

10 May 2015

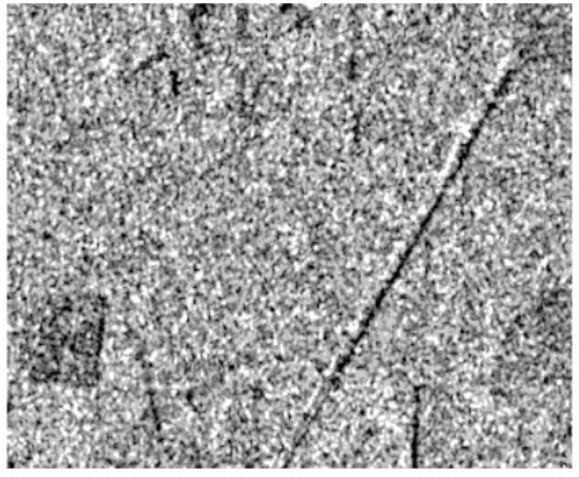

1 October 2016

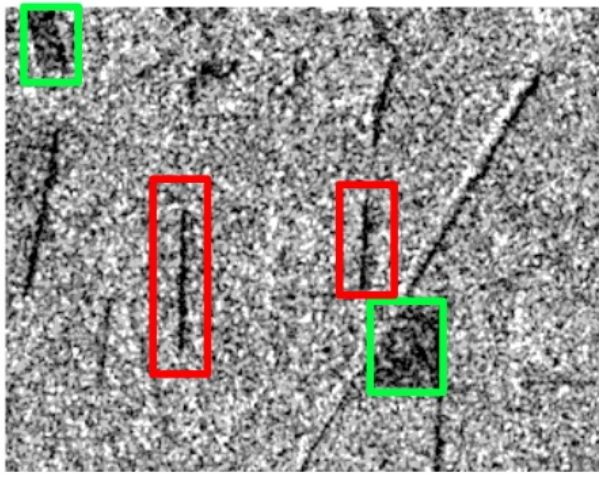

Recent logging
Older logging shadow edge

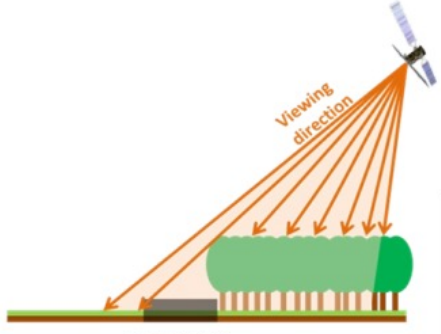

10 m resolution,
>90% accuracy (Peru, Gabon, French Guiana, Brasil and Vietnam)

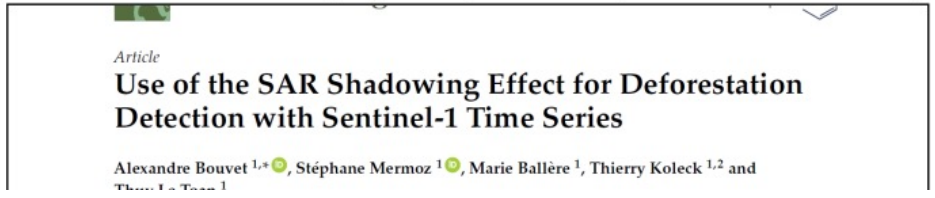

Article

Use of the SAR Shadowing Effect for Deforestation Detection with Sentinel-1 Time Series

Alexandre Bouvet [1,*], Stéphane Mermoz [1], Marie Ballère [1], Thierry Koleck [1,2] and

CESBIO

4.9 Near-Real Time deforestation monitoring using S1

https://www.spaceclimateobservatory.org/tropisco-amazonia

Remote Sensing of Environment
Volume 252, January 2021, 112159

SAR data for tropical forest disturbance alerts in French Guiana: Benefit over optical imagery

Marie Ballère [a, b, c], Alexandre Bouvet [d], Stéphane Mermoz [d, e], Thuy Le Toan [d], Thierry Koleck [a], Caroline Bedeau [f], Mathilde André [f], Elodie Forestier [f], Pierre-Louis Frison [c], Cédric Lardeux [g]

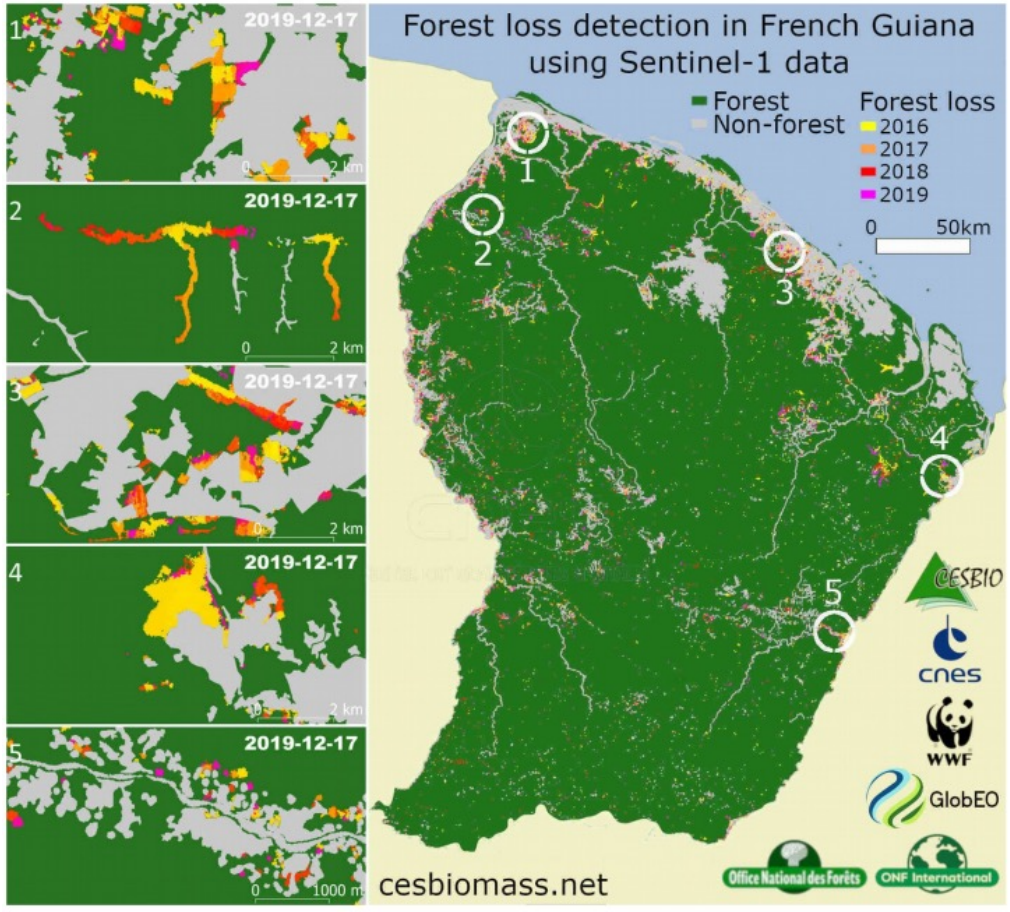

Drivers: gold mining, smallholder agriculture and forest exploitation

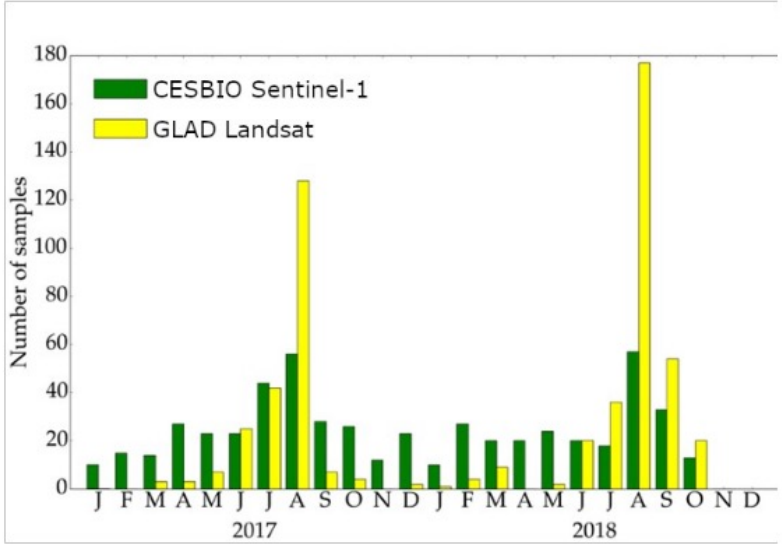

Validated using **1 867 in situ plots** covering 2 124.5 ha: **UA of 96.2%** and **PA of 81.5%**

Monitoring forest disturbance in tropical regions

https://www.spaceclimateobservatory.org/tropisco-amazonia

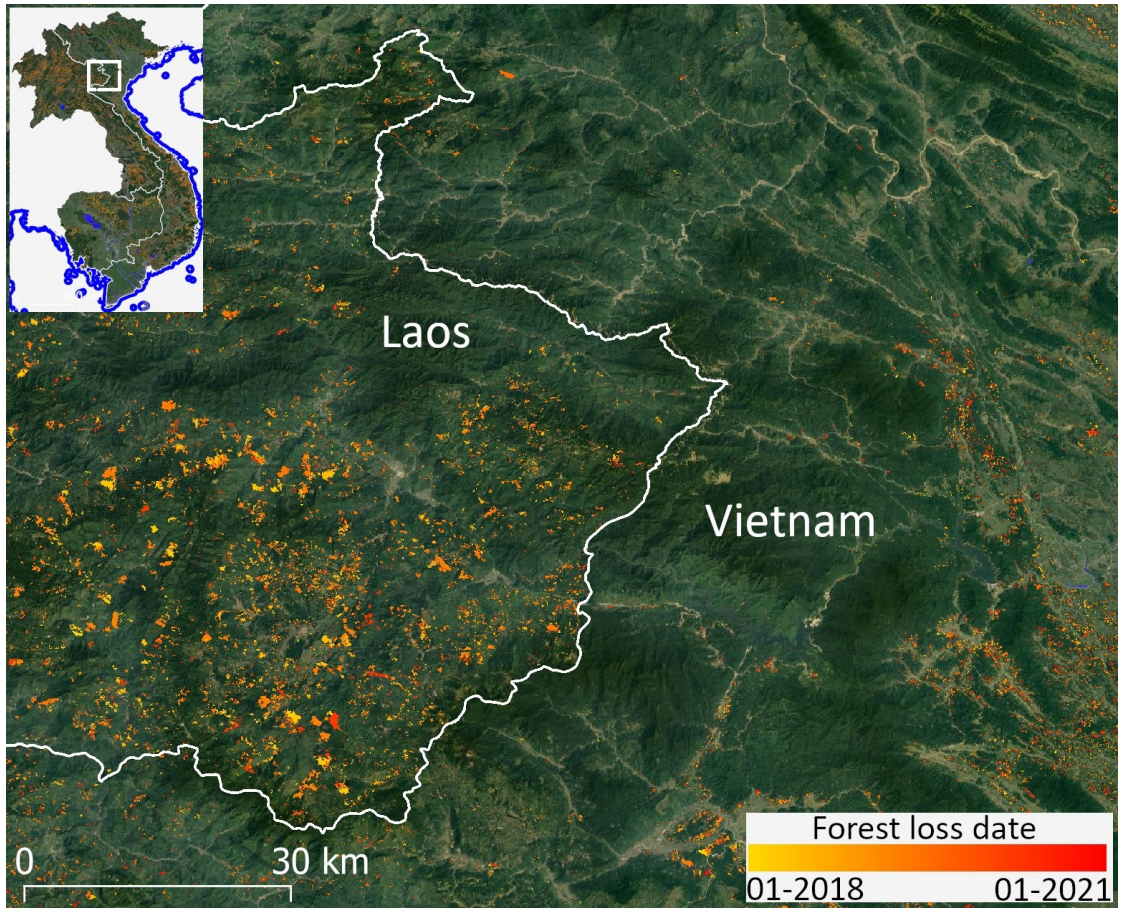

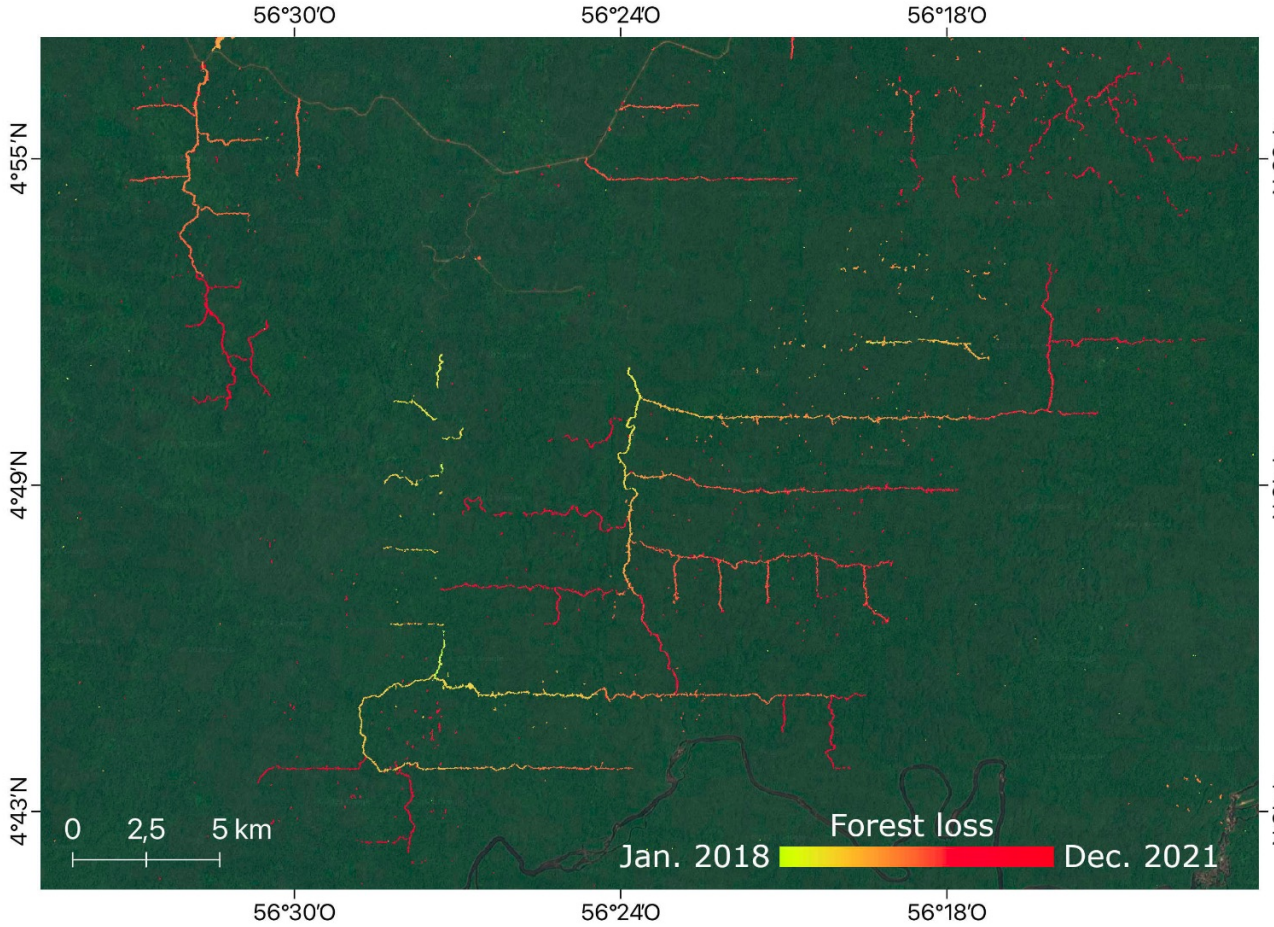

5. Training of young scientists

- European Young scientists contributions in Dragon 5

Name	Institution	Poster title	Contribution
1. P.A. BOU	CESBIO & ONERA	3-D SAR imaging of forests from space at higher frequency bands using incoherent bistatic tomography Concepts and validation using the TomoSense campaign (2022)	Tomography at higher frequencies from space(2years)
2. Y. XI	CSU (China) & CESBIO	/	BIOMASS DB PolinSAR (Chines-French co-supervision) (arrived in Feb. 2022)
3. M. BOTTANI	ISAE-SUPAERO & CESBIO	/	Deforestation monitoring using S1 & S2. Beginning in Nov. 2022

5. Training of young scientists

- Chinese Young scientists contributions in Dragon 5

Name	Institution	Poster title	Contribution including period of research
1. Kunpeng Xu	IFRIT CAF	Research On Forest Height Extraction Method Based On Multi-band InSAR Data(2022)	Forest height estimation utilizing the penetration difference between P- and X-band InSAR data. (3years)
2. Yaxiong Fan	IFRIT CAF	Forest Height Estimation Using Short-baseline PolinSAR Data(2022)	Potential of time series short-baseline PolInSAR data for forest height (3years)
3. Yunmei Ma	IFRIT CAF	Evaluation of Forest Aboveground Biomass Estimation Capacity of X-band and P-band Interferometric SAR Data (2023)	Forest AGB estimation using X and P band InSAR data: method validation. (2years)
4. Ni Jun	BUCT	A Covariance-based Feature Extraction Method for Temporal PolSAR Imageries(2021)	Multi-temporal PolSAR image classification(3years)
5. Zhiyuan Lin	BUCT	A Temporal Polarization SAR Classification Method Based on Polarimetric-Temporal Feature Selection(2022)	Time series PolSAR classification(2years)
6. Gao Li	BUCT	A Multi-Temporal Polarimetric SAR Classification Method Based on Time-Variant Scattering Features	PolSAR image classification(1years)
7. Shuo Li	BUCT	Multi-Band CARSS Airborne PolSAR Image Classification	Muli-band PolSAR classificaiton(1years)
8.. Yuming Du	BUCT	Temporal Dual-polarization SAR Crop Classification Based on Coherence Optimization	Multi-temporal dul-pol classification using coherence(1years)

5. Training of young scientists

- PolSARpro and community events

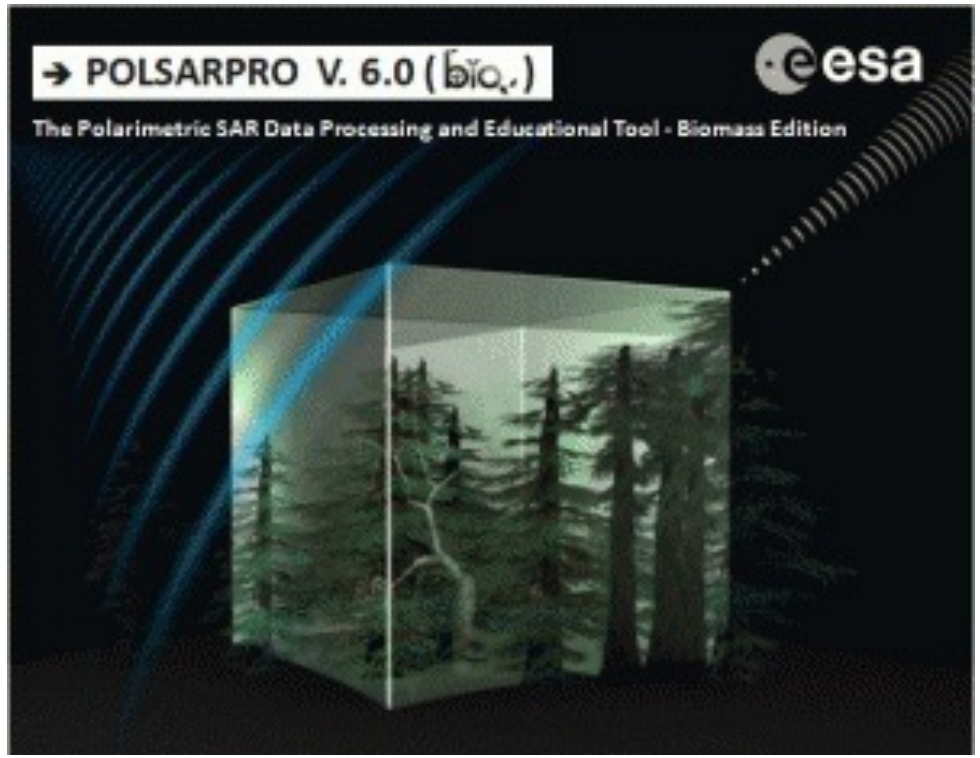

U. Rennes 1, IETR, E. Pottier

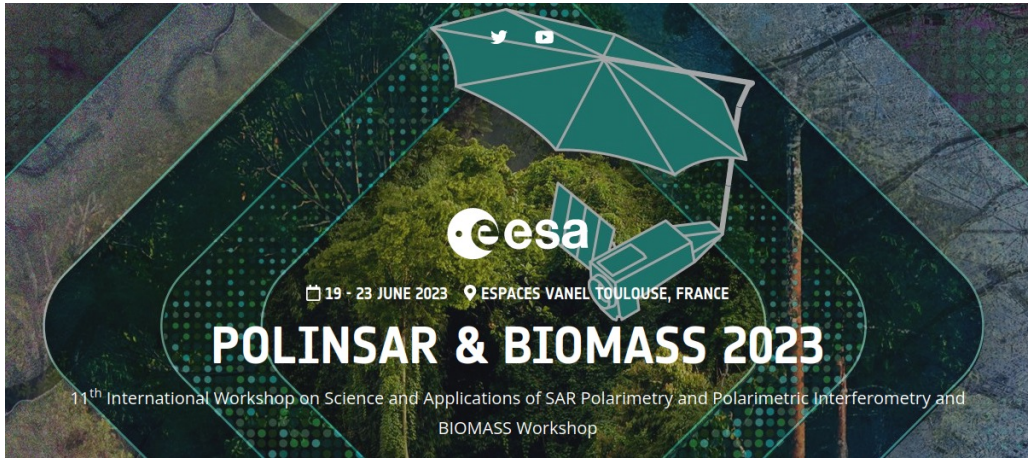

- **ESA PolinSAR & BIOMASS workshop**

  Toulouse, France, 19-23 june 2023

- **ESA SAR polarimetry training**

  Toulouse, France, 12-16 june 2023

6. Peer reviewed publications

■Published 25 papers

1. Qiang Yin, Junlang Li, Yongsheng Zhou, Deliang Xiang & Fan Zhang. Adaptive weighted learning for vegetation contribution in soil moisture inversion using PolSAR data, International Journal of Remote Sensing, 2022, 43:9, 3190-3215.
2. Qiang Yin; Jie Xu; Deliang Xiang*; et al. Polarimetric Decomposition With an Urban Area Descriptor for Compact Polarimetric SAR Data. IEEE Journal of Selected Topics in Applied Earth Observations and Remote Sensing, 2021, 14: 10033-10044.
3. Qiang Yin; Junlang Li; Fei Ma*; et al. Dual-Channel Convolutional Neural Network for Bare Surface Soil Moisture Inversion Based on Polarimetric Scattering Models. Remote Sensing, 2021, 13(22): 4503.
4. Ying Luo；Qiang Yin*；Fei Ma；A Discrimination Method of Water and Shadow Areas Based on Polarization Entropy of Sentinel-1 Data，IEEE International Geoscience and Remote Sensing Symposium (IGARSS), 2022.07.17-22.
5. Qiang Yin, Zhiyuan Lin, Wei Hu, Carlos López-Martínez, Jun Ni and Fan Zhang*, Crop Classification of Multitemporal PolSAR Based on 3-D Attention Module With ViT, IEEE Geoscience and Remote Sensing Letters, vol. 20, pp. 1-5, 2023.
6. Shasa Deng; QiangYin*; Fan Zhang; Xinzhe Yuan; A Ship Ghost Interference Removal Method Based on GaoFen-3 Polarimetric SAR Data, IEEE International Geoscience and Remote Sensing Symposium (IGARSS), 2022.07.17-22.
7. Zhiyuan Lin; Qiang Yin*；Yongsheng Zhou；Jun Ni；Fei Ma; Time-series PolSAR Crop Classification Based on Joint Feature Extraction, IEEE International Geoscience and Remote Sensing Symposium (IGARSS), 2022.07.17-22.
8. Zhao Lei, Chen Erxue, Li Zengyuan, et al. A New Approach for Forest Height Inversion Using X-Band Single-Pass InSAR Coherence Data. IEEE Transactions on Geoscience and Remote Sensing, 2022, 60: 5206018. DOI:10.1109/TGRS.2021.3072125
9. Xu, K.; Zhao, L.; Chen, E.; Li, K.; Liu, D.; Li, T.; Li, Z.; Fan, Y. Forest Height Estimation Approach Combining P-Band and X-Band Interferometric SAR Data. Remote Sens. 2022, 14, 3070. https://doi.org/10.3390/rs14133070
10. Zhao Lei, Chen Erxue, Li Zengyuan et al. The Improved Three-Step Semi-Empirical Radiometric Terrain Correction Approach for Supervised Classification of PolSAR Data [J]. Remote Sensing, 2022，14(3):595. DOI:10.3390/rs14030595
11. Wan, X.; Li, Z.; Chen, E.; Zhao, L.; Zhang, W.; Xu, K. Forest Aboveground Biomass Estimation Using Multi-Features Extracted by Fitting Vertical Backscattered Power Profile of Tomographic SAR. Remote Sens. 2021, 13, 186
12. Ning Liu, Xinwu Li, Xing Peng, Wen Hong, SAR Tomography Based on Atomic Norm Minimization in Urban Areas. Remote Sensing. 2022, 14, 3439.
13. Xing Peng, Youjun Wang, Shilin Long, Xiong Pan, Jianjun Zhu, Xinwu Li. Underlying Topography Inversion Using TomoSAR Based

6. Peer reviewed publications

14. Mor Diama Lo, Matthieu Davy, Laurent Ferro-Famil. Low-Complexity 3D InISAR Imaging Using a Compressive Hardware Device and a Single Receiver. Sensors, 2022, 22 (15), pp.5870. ⟨10.3390/s22155870⟩.
15. Yen-Nhi Ngo, Yue Huang, Dinh Ho Tong Minh, Laurent Ferro-Famil, Ibrahim Fayad, et al.. Tropical forest vertical structure characterization: From GEDI to P-band SAR tomography. IEEE Geoscience and Remote Sensing Letters In press, 19, pp.1-1. ⟨10.1109/LGRS.2022.3208744⟩. ⟨hal-03793062⟩, IEEE - Institute of Electrical and Electronics Engineers,
16. Mhamad El Hage, Ludovic Villard, Yue Huang, Laurent Ferro-Famil, Thierry Koleck, et al.. Multicriteria Accuracy Assessment of Digital Elevation Models (DEMs) Produced by Airborne P-Band Polarimetric SAR Tomography in Tropical Rainforests. Remote Sensing, 2022, 14 (17), pp.4173.
17. Colette Gelas, Ludovic Villard, Laurent Ferro-Famil, Laurent Polidori, Thierry Koleck, et al.. Multi-Temporal Speckle Filtering of Polarimetric P-Band SAR Data over Dense Tropical Forests: Study Case in French Guiana for the BIOMASS Mission. Remote Sensing, 2021, 13 (1)
18. Ray Abdo, Laurent Ferro-Famil, Frédéric Boutet, Sophie Allain-Bailhache. Analysis of the Double-Bounce Interaction between a Random Volume and an Underlying Ground, Using a Controlled High-Resolution PolTomoSAR Experiment. Remote Sensing, 2021, 13 (4)
19. Y. Huang, Q. Zhang, and L. Ferro-Famil, "Forest Height Estimation Using a Single-Pass Airborne L-Band Polarimetric and Interferometric SAR System and Tomographic Techniques," Remote Sensing, vol. 13, no. 3, p. 487, Jan. 2021
20. Morin D, Planells M, Baghdadi N, Bouvet A, Fayad I, Le Toan T, Mermoz S, Villard L. Improving Heterogeneous Forest Height Maps by Integrating GEDI-Based Forest Height Information in a Multi-Sensor Mapping Process. Remote Sensing. 2022; 14(9):2079
21. Emma Bousquet, Arnaud Mialon, Nemesio Rodriguez-Fernandez, Stéphane Mermoz, Yann Kerr. Monitoring post-fire recovery of various vegetation biomes using multi-wavelength satellite remote sensing. Biogeosciences, European Geosciences Union, 2022, 19 (13), pp.3317-3336
22. Salma El Idrissi Essebtey, Ludovic Villard, Pierre Borderies, Thierry Koleck, Benoît Burban, et al.. Long-Term trends of P-band temporal decorrelation over a tropical dense forest-experimental results for the BIOMASS Mission. IEEE Transactions on Geoscience and Remote Sensing, Institute of Electrical and Electronics Engineers, 2022, 60, ⟨10.1109/TGRS.2021.3082395
23. Yang, H, Ciais, P, Wang, Y, et al. Variations of carbon allocation and turnover time across tropical forests. Global Ecol Biogeogr. 2021; 30: 1271– 1285.
24. Marie Ballère, Alexandre Bouvet, Stéphane Mermoz, Thuy Le Toan, Thierry Koleck, Caroline Bedeau, Mathilde André, Elodie Forestier, Pierre-Louis Frison, Cédric Lardeux, SAR data for tropical forest disturbance alerts in French Guiana: Benefit over optical imagery, Remote Sensing of Environment, Volume 252, 2021
25. Papathanassiou, K.P. et al. (2021). Forest Applications. In: Hajnsek, I., Desnos, YL. (eds) Polarimetric Synthetic Aperture Radar. Remote Sensing and Digital Image Processing, vol 25. Springer, Cham. https://doi.org/10.1007/978-3-030-56504-6_2

Publications

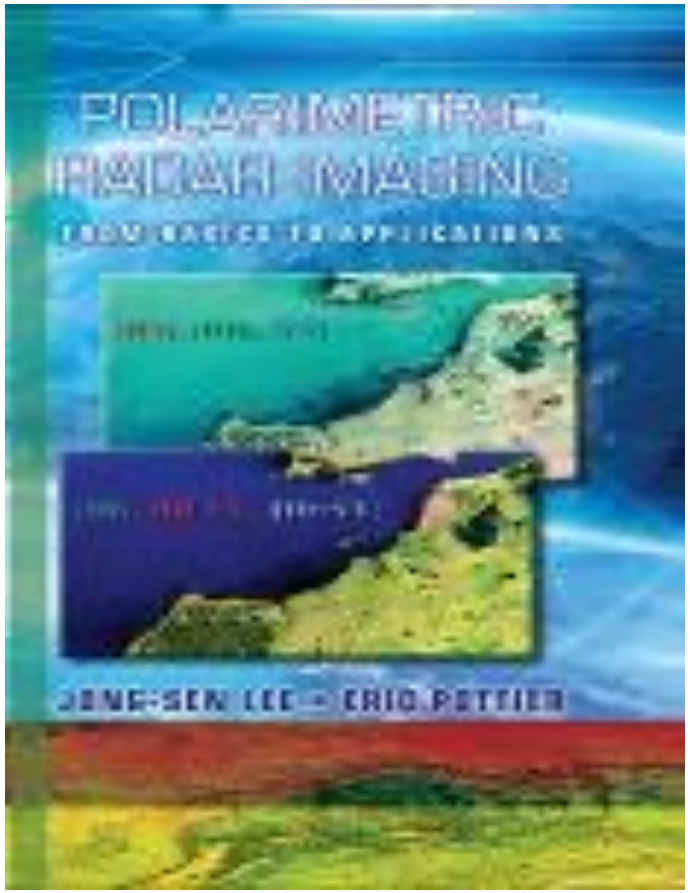

Polarimetric Radar Imaging: From basics to applications
Jong-Sen LEE – Eric POTTIER

2nd Edition in Chinese by
Wen Hong, Yang Li, Qiang Yin
Publishing House of Electronics Industry, 2021.7

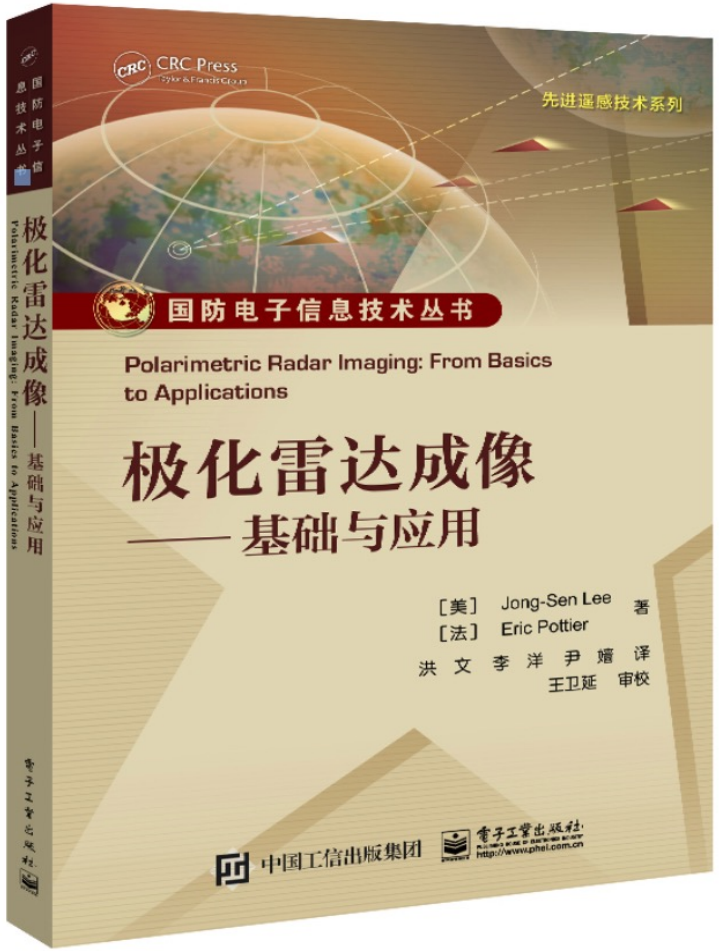

7. Schedule, planning & contribution of 2024

- Tomo-SAR forest imaging methods in high relief region using airborne MB-PolInSAR data of China test sites
- BIOMASS forest product validation if launched in 2024
- Young scientist exchanges
- DRAGON5 final results summary and joint proposal for DRAGON6

Thanks